

A MINERALOGICAL STUDY
OF SCAPOLITE

A MINERALOGICAL STUDY

OF SCAPOLITE

By

DAVID RODERICK HAUGHTON B.Sc. (Eng.)

A Thesis

Submitted to the Faculty of Graduate Studies

in Partial Fulfilment of the Requirements

for the Degree

Master of Science

McMaster University

October 1967

ABSTRACT

Eight new scapolite analyses are presented. Determinations of refractive index, specific gravity, and lattice parameters are examined in conjunction with data available in five recent analyses. Particular reference is made to the regular variation of per cent Cl_2 , CO_2 and SO_3 as a function of mole per cent meionite and the relation of these components to scapolite stability. End member formulae describing the composition of scapolite are developed.

These scapolite samples are used in conjunction with synthetic plagioclase standards to obtain forty three electron microprobe analyses of scapolite-plagioclase pairs and twenty seven separate analyses of scapolite. The former analyses indicate that scapolite from amphibolite and granulite facies is generally more calcium-rich than the coexisting plagioclase.

A petrographic study indicates that scapolite associated with the above grade of metamorphism is indicative of a volatile rich environment typified in the amphibolite facies by the assemblage sphene-pyroxene-scapolite.

ACKNOWLEDGMENTS

The author would like to express thanks to Dr. D.M. Shaw, thesis supervisor and Dr. H. P. Schwarcz for their excellent and constructive criticisms during the writing of the thesis; to Mr. J. Muysson, analyst for his superb work; to Mr. Harry Walker for his assistance in probe studies; to Mr. F. Tebay for his cooperation during x-ray studies; to Mr. D. Falkiner for his aid in preparing thin sections; to my fellow students who freely gave advice, in particular Mr. B. Robertson for his contribution to my FORTRAN programs; to those who so freely supplied samples to be studied and finally to my wife who with infinite patience typed the following manuscript.

TABLE OF CONTENTS

Introduction	Page 1
Review of Scapolite Mineralogy	3
General	3
Structure	5
Petrography of Scapolite Rocks	8
Association of Scapolite and Plagioclase	11
Synthetic Scapolite	13
Crystal Chemistry	15
Choice and Preparation of Standards (Scapolite)	15
Criteria for Selection	15
Plagioclase Standards	17
Determination and Discussion of Chemical Properties of Scapolite Standards	20
End Member Formulae	44
Determination and Discussion of Physical Properties of Scapolite Standards	48
Specific Gravity	48
Refractive Index	54
Lattice Parameter Determination	55
Probe Studies	64
The Electron Probe Microanalyzer	64
General	64

TABLE OF CONTENTS CONT'D

Specifics	Page 65
Electron Optics	65
Light Optics	68
X-ray Optics	68
Specimen Chamber and Vacuum System	69
Analyzing Electronics	70
Analytical Procedure	70
Mounting of Standards	72
Preparation of Polished Thin Sections	75
Calibration Curves and Determination of Homogeneity	77
Scapolite Standards	77
Plagioclase Standards	89
Sample Sources	89
Plagioclase Scapolite Analysis	96
Discussion of Plagioclase-Scapolite Analysis	96
The Equilibrium Coefficient	104
Discussion of Scapolite Analysis	106
Extremal States	107
Wavelength Shifts	107

TABLE OF CONTENTS CONT'D

Petrology	Page 111
Petrogenesis of Scapolite	111
Mineral Facies	118
Conclusions	121
Bibliography	123

LIST OF TABLES

	Page
Table 1 Scapolite Mineral Assemblages and Localities	18
2 Scapolite Analyses	21
3 Gram Atom Values and Corresponding Mole Per Cent Meionite	24
4 Solution of Linear Regression Equations for 0 and 100 Mole Per Cent Meionite Values	45
5 Conversion from Weight Per Cent to Gram Atom Values	46
6 Specific Gravity Determinations	50
7 Optical Parameters	54
8 Axial Parameters hkl, and Respective θ Values	59
9 Localities of Scapolite Bearing Rocks	91
10 Coexisting Scapolite and Plagioclase Analysis by Microprobe	97
11 Scapolite Analyses by Microprobe	101

LIST OF FIGURES

Fig. 1	The Crystal Structure of Marialite	Page 7
2	Mole % Meionite vs Weight % Cl	29
3	Mole % Meionite vs Weight % SO ₃	31
4	Mole % Meionite vs Weight % CO ₂	33
5	Mole % Meionite vs Weight % Na ₂ O	35
6	Mole % Meionite vs Weight % CaO	37
7	Mole % Meionite vs Weight % Al ₂ O ₃	39
8	Mole % Meionite vs Weight % SiO ₂	41
9	Specific Gravity vs Mole % Meionite	53
10	Optical Properties of Scapolite	57
11	Unit Cell Parameters	63
12	A Schematic Diagram of the Electron Probe Microanalyzer	67
13	Calibration Curve Utilizing Mica Crystal	79
14	Calibration Curve Utilizing Quartz 1011 Crystal	81
15-24	Scans Across Scapolite Standards	84-88
25	Mole % Meionite vs Mole % Anorthite	103
26	Mole % Meionite vs Frequency of Analysis	109
27	Facies Diagrams for Scapolite Assemblages	120

LIST OF PLATES

Plate 1	Microanalyzer Standard Holders	Page 74
2	Anorthosite IM-3 Illustrating initial stages of scapolitization	111
3	Anorthosite IM-3 Illustrating intersertal scapolitization	112
4	Anorthosite S-44 Illustrating equigranular texture	113
5	Anorthosite S-54 Illustrating equigranular and replacement textures	114
6	Hornblende-Scapolite-Sphene Plagioclase gneiss CA 76	114
7	Scapolite-Plagioclase-Hornblende Gneiss, poikiloblastic texture	115
8	Paramphibolite Illustrating stringers of scapolite	116
9	Paramphibolite Illustrating bands of scapolite	117

INTRODUCTION

Controversy regarding the role of scapolite in metamorphic processes is present in the recent works of Barth (1952); Fyfe, Turner and Verhoogen (1958); Marakushev (1964); and Shaw (1960). Therefore the primary purpose of this thesis is to delineate the fundamental properties and the paragenesis of scapolite.

Little is known of the conditions necessary for the stability of scapolite. Thus any delineation of scapolite stability requirements will further advance the geologist's knowledge of metamorphic environments.

Scapolite, a sodium calcium aluminum silicate which is predominately found in rocks of the amphibolite facies, contains appreciable amounts of the volatiles CO_2 , Cl_2 and SO_3 . It has become increasingly evident that the role of these volatiles and others such as oxygen and hydrogen is of paramount importance in metamorphic processes. Scapolite in abundance is certainly characteristic of a specific orogenic environment, one

presumably rich in CO_2 , Cl_2 , and SO_3 .

The role of the electron probe in this study must be emphasized. It is well-suited for studying the relationships between scapolite and coexisting plagioclase, which constitute one of the aims of this study.

To conduct a mineralogical study of scapolite thirteen scapolite samples have been studied in detail, undertaking chemical and x-ray analysis, specific gravity and refractive index determinations.

REVIEW OF SCAPOLITE MINERALOGY

General.

The most comprehensive papers on scapolite to this date have been those published by D.M. Shaw (1960) and a Ph.D. thesis by J.J. Papike (1964). Shaw reviewed intensively the previous work and general mineralogy of scapolite, as well as conducting research on the trace element distribution, petrology and general geochemistry of this mineral.

Papike conducted a detailed structural study of a 19.4% meionite scapolite.

Part 1 of Shaw's paper reappraised earlier views by the authors Tschermak (1883), Adams (1879), Brauns (1914), Sundius (1915, 1916, 1919), Shannon (1921), Winchell (1924), Barth (1924, 1927a, 1927b, 1930), Gossner and Bruckl (1927), and Strunz (1949). Shaw agrees with many of their findings in particular that scapolite contains the anions $\text{CO}_3^{=}$, $\text{SO}_4^{=}$, Cl^- and possibly F^- and OH^- as essential components. Shaw writes the general formula of scapolite as $\text{W}_4\text{Z}_{12}\text{O}_{24} \cdot \text{R}$, where W is mainly Ca, Na and K, Z is Si and Al. R is

either a) CO_3 , SO_4 , O_2H_2 , Cl_2 or F_2 for meionite (the calcium rich end member) or b) Cl , F , HCO_3 , HSO_4 or OH for marialite (the sodium rich end-member). The nomenclature is accepted as:

marialite, $\text{Me}_0\text{-Me}_{20}$; dipyre, $\text{Me}_{20}\text{-Me}_{50}$; mizzonite, $\text{Me}_{50}\text{-Me}_{80}$ meionite, $\text{Me}_{80}\text{-Me}_{100}$. It was noted by Shaw that pure marialite has not been found and that 80% marialite is apparently the maximum attained. Shaw's study of 136 analyses further established limits on the chemical and physical parameters as well as confirming and suggesting trends in some of these. It was noted that the mean index of refraction varied approximately linearly as a function of per cent meionite, from 1.535 (marialite) to 1.585 (meionite). Specific gravity varied from 2.692 to 2.615 and showed a tendency to increase when plotted against mole per cent meionite, although scatter was considerable.

Papike (1964) stated on the basis of his structural studies that the formula for the meionite end member $\text{Ca}_4(\text{Al}_6\text{Si}_6\text{O}_{24})\text{CO}_3$ was in error, although the marialite formula was acceptable. The samples studied by Papike were M 730, Q 85, Q 19D-S, Q 87, ON 6A and ON 8. Five

of these samples contributed by D.M. Shaw are used in the present study.

On the basis of a and c determinations Eugster, Prostka and Appleman (1962), illustrated clearly that the regular increase in unit cell volume with increasing percentage meionite could be used to determine the composition of unanalyzed scapolite. This work was confirmed by Papike (op.cit.), that is, that a-values in natural scapolite increase regularly with increasing meionite content. The value of c remains approximately constant, regardless of scapolite composition. Infrared absorption analysis was used by Papike to indicate that carbon was present in the scapolite structure in $\text{CO}_3^{=}$ groups. A study by Schwarcz and Speelman (1965) agreed with the latter conclusion.

Structure.

Figure 1 illustrates the structure of marialite-rich scapolite. The framework of the structure is composed of (Si,Al)O tetrahedra forming rings of two types: a plane passing through these rings would be parallel to (001). Type 1 is composed of 4 tetrahedra, each joined at two corners, with one edge parallel to the c axes. Type 2

FIGURE 1

The crystal structure of marialite
(after J.J. Papike).

FORMULA: $\text{Na}_4\text{Al}_3\text{Si}_9\text{O}_{24}\text{Cl}$

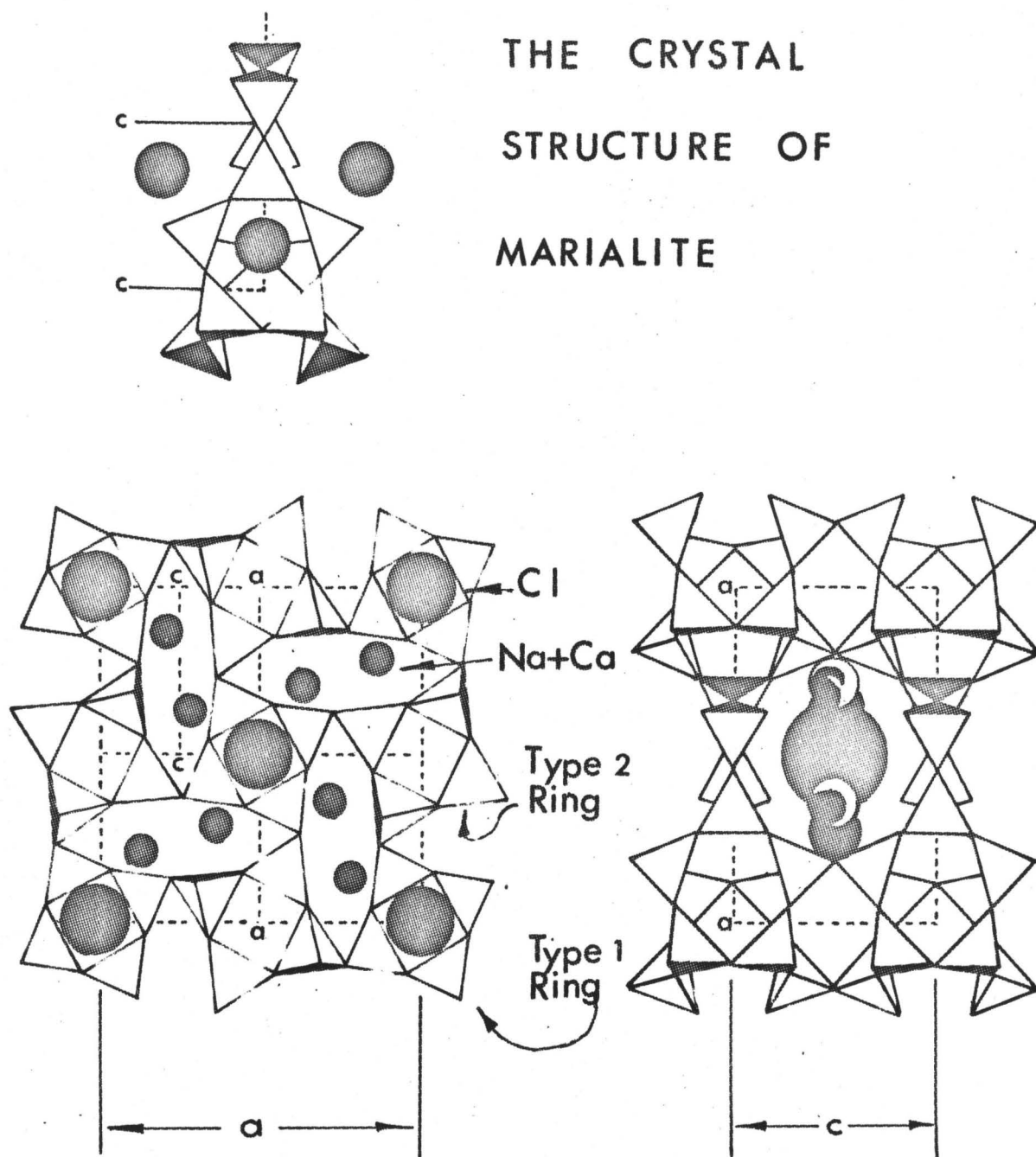


FIGURE 1

is composed of 4 tetrahedra pointing alternately up and down. The framework of these rings forms a tetragonal structure having a large central opening which is surrounded by four oval cavities. These cavities are elongated parallel to c. The longitudinal axis of each oval is parallel to one of the four sides of a section perpendicular to c. The large central opening in marialite is occupied by Cl and the oval vertical cavities are occupied by (Na, Ca) ions. Papike (1964) notes that each (Cl^- , $\text{SO}_4^{=}$, $\text{CO}_3^{=}$) ion is coordinated by 4 (Na,Ca) atoms and 5 oxygen atoms.

Petrography of Scapolite Rocks.

From a study of the mineral facies in which scapolite appeared it is evident that scapolite, although found in all facies from zeolitic to granulite as well as in some hornfels facies assemblages, is most prevalent in the upper amphibolite facies. The assemblage scapolite-pyroxene-sphene is a characteristic calcareous assemblage of world wide distribution. This assemblage appears to represent a particular conjunction of geological conditions. The conditions for the existence of scapolite are observed to cover a wide P,T field coupled with pegmatitic, pneumatolytic or hydrothermal action.

The following briefly describes the main modes of occurrence of scapolite (after Shaw 1960)

- a) in blocks ejected from volcanoes by volcanic action;
- b) in contact skarns or tactites where sedimentary marbles have been influenced by nearby plutonic bodies;
- c) in altered igneous rocks especially gabbro and diabase altered by the effect of hydrothermal or pneumatolytic fluids (possibly also by ground water action, as claimed by LaCroix in the Pyrenees);
- d) in metamorphic rocks of regional distribution especially marbles, greenstones, calcareous gneisses and granulites but also in pelitic and psammitic varieties;
- e) in metamorphosed salt deposits. (Serdyuchenko 1955).

To the above list might be added primary scapolite, such as that occurring in granulite inclusions and in breccia and basalt filled pipes of eastern Australia, (Lovering 1964). The suggestion was made by Lovering (1964), on the basis of the study of such rocks, that within the granulite facies there appears to be a progressive increase in the sulphur content of scapolite in equilibrium with sulphur-rich minerals with increasing metamorphic grade.

Of the above, b) and d) are perhaps the most common locales for scapolite. In the amphibolite facies regionally metamorphosed rocks are locally associated

with scarns. Some skarns have zoned structures as described from Gib Lake (Shaw, Schwarcz and Sheppard, 1965); progressing outwards from the centre the following sequence was observed:

1) blue scapolite 2) pargasite-albite intergrowth
3) phlogopite 4) serpentinized forsterite-dolomite marble. Shaw et al. stated that these skarns appear to be products of partial metasomatism with H, Cl, C, F, S, Na and K behaving as perfectly mobile components with fixed chemical potentials. The elements Mg, Si and Al were regarded as slowly diffusing determining inert components while Ca was considered as an excess component.

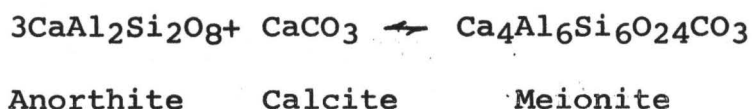
A zoned dike or skarn having similar mineralogy occurs in an area of predominately migmatic gneisses in Finland. From the core it has the following sequence:
1) scapolite 2) tremolite 3) phlogopite 4) wall rock (crystalline limestone.) It is ascribed by Harme (1965) to injection by alkali granitic material relatively poor in silica.

In a detailed study of the petrology and geochemistry of some Grenville skarns (Shaw, Moxham, Filby and Lapkowsky, 1963) it was demonstrated for numerous localities

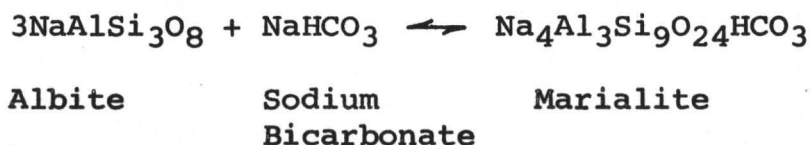
in S.W. Quebec and S.E. Ontario that skarns show petrographic transition to normal Grenville amphibolites, marbles, granites gneisses and pegmatites. The skarns appear to have been formed by in situ metasomatism, metamorphic differentiation, vein and pegmatitic deposition, bulk flow and injection. It is stated also that skarn formation was presumably the last event recorded in the Pre-Cambrian history of this region. The appearance of the assemblage scapolite-diopside-sphene is again noted and recommended to denote a new meta-facies characterized by high CO_2 and Cl_2 and intermediate H_2O pressures. Environmental conditions were those resulting from a burial of 20-25Km and a temperature of 300-400°C.

Association of Scapolite and Plagioclase.

Turner and Verhoogen (1951, p. 390) state that scapolite is always richer in calcium than coexisting plagioclase. Barth (1952) invokes the following two equations as examples of scapolitization of plagioclase.



and



His tentative equilibrium diagram shows scapolite enriched in calcium with respect to plagioclase by as much as 60 mole per cent and generally richer in Ca by 25 mole per cent meionite. Marakushev (1964) claimed that when conditions approached equilibrium as found in metamorphic rocks of "deep seated" Precambrian complexes a definite relationship was established between the composition of plagioclase and scapolite. Applying Korzhinskii's method of analysis of extremal systems to compositional data which had been obtained from the literature Marakushev reached the following conclusions:

1. In the two phase assemblage plagioclase-scapolite; scapolite is generally more calcic than the associated plagioclase.
2. The assemblage scapolite-plagioclase-quartz-calcite has an extremum at which plagioclase and scapolite have the respective compositions An_{50} , Me_{60} . (The extremal conditions were to be found in marbles metamorphosed at high temperatures and pressures. This is because at the extremum a_{CO_2} is maximized.)
3. The three phase assemblage scapolite-plagioclase-calcite forms at low or moderate chlorine activity. The assemblages scapolite-quartz-plagioclase and scapolite-quartz-calcite form only at high chlorine activity.

Marakushev stresses throughout his paper that the association of chlorine-rich or sulphur-rich scapolite

is dependent upon rock type.

Shaw (1960) however, presented data illustrating that scapolite was not always richer in calcium than co-existing plagioclase and that there was no regular relationship between scapolite and plagioclase.

Synthetic Scapolite.

Eugster and Prostka (1960) synthesized marialite from dry mixtures of $\text{Na}_2\text{O} \cdot 6\text{SiO}_2$, Al_2O_3 and NaCl at one atmosphere pressure between 700° and 850°C . Meionite was also produced at 850°C and one atmosphere from SiO_2 , Al_2O_3 and CaCO_3 . Seeding was necessary. The authors also note that marialite melts incongruently to albite plus liquid at $860^\circ\text{C} \pm 10^\circ\text{C}$.

A comparison of cell dimensions and unit cell volume (Eugster, Prostka and Appleman 1962) illustrated that the cell dimensions of some synthetic scapolites did not agree with those of natural scapolites.

The mean values of the cell dimensions estimated by Eugster et al from a range of values of different samples are: synthetic marialite, $a = 12.064$, $c = 7.514$, cell volume = 1093.5; synthetic meionite, $a = 12.174$, $c = 7.652$, cell volume = 1134.1 (all values are in angstrom units).

The above data illustrates that both a and c are larger in synthetic meionite than in synthetic marialite.

R.C. Speed of the Jet Propulsion Laboratory, California Institute of Technology has attempted to synthesize sodic scapolite over the past several years but has only been able to obtain crystal growth in seeded runs (personal communication).

It appears that all synthetic scapolites produced have required seeding.

CRYSTAL CHEMISTRY

Choice and Preparation of Standards (Scapolite).

Since synthetic standards were not available natural scapolite standards have been used in this study.

Criteria for Selection: The following factors must be considered when choosing standards:

1. Standards should cover a large range of chemical composition.
2. Standards should be numerous enough to allow for internal checks and to obtain good working curves.
3. Standards should be unweathered.
4. Standards should be homogeneous, that is lacking inclusions and showing no zonation.
5. Sufficient amounts of each standard should be available for further study.
6. Standards should be obtained from a wide range of geologic environments to prevent the effects of local variation in physical and chemical parameters from producing misleading results.
7. If possible, rocks from which the standards are obtained should be lacking in minerals having physical properties similar to scapolite. Such minerals would be difficult to separate.

After megascopic examination thirty-three scapolite bearing rocks were first crushed using a jaw crusher, (all fines were discarded to prevent contamination of the bulk samples.) Then with steel mortar and pestle the rock was broken into particles having an average diameter of 3 mm. from which numerous scapolite grains were hand picked. These grains were further crushed and sieved. The -100, +200 fraction was retained, washed to remove fines and then passed through a Frantz magnetic separator. A 15° x 15° slope and a current of 1.5 amps. separated the majority of the scapolite from the mafic minerals. That portion of the powder containing abundant scapolite was rerun under a variety of slope and current combinations to further purify the scapolite portion. Finally, the least magnetic fraction was washed and retained for further processing. Heavy liquid separation was used to further purify the scapolite powder. The specific gravity of a tetrabromethane mixture was adjusted, first so that scapolite would barely float; secondly so that it would sink. This procedure was repeated until the scapolite fraction was relatively pure. A time interval of eight hours was required for separation at each stage. The floating or sinking portion

was frequently stirred to prevent foreign minerals from becoming entrapped by surrounding scapolite grains. Since a small proportion of scapolite was discarded due to density differences, the sample retained should possess consistent and uniform chemical and physical properties. It was assumed that the grains which were retained for use as probe standards would represent this most abundant fraction. After washing thoroughly with acetone the remaining sample was placed in a covered beaker containing dilute acetic acid for a period of eight hours to remove included calcite. The sample was then washed with acetone, dried and finally examined by means of a petrographic microscope. From the thirty-three samples examined, thirteen which were thought to be the purest were kept for detailed study. Included in these thirteen were ON 8, ON 6A, Q 87 and Q 85 which have been studied in detail by Shaw (1960) and later by Papike (Ph.D. thesis, 1964). G.L. is described by Shaw et al (1965). Table 1 lists the mineral assemblages associated with these thirteen scapolites.

Plagioclase Standards.

The plagioclase standards used were synthetic glass samples contributed by D. Lindsley, Geophysical Laboratory Washington. These cover the range of plagioclase composition

TABLE 1

Scapolite Mineral Assemblages and Localities

SAMPLE	MINERAL ASSEMBLAGE	COMMENTS ON POWDER	LOCALITY
ON 8	Scapolite Feldspar Nepheline	Slight fibrous alteration and staining	Glamorgan Twp. Ontario
GL	Scapolite Amphibole Mica Plagioclase	1% feldspar	Pontefract Twp. Quebec
ON 6A	Scapolite Pyroxene Sphene		Monmouth Twp. Ontario
ON 70	Scapolite		Mpwapwa, Tanzania. (gift of Dr. F.W. Solesbury)
ON 3B	Scapolite Pyroxene	Very slight staining on some grains	Lyndoch Twp. Ontario.
Q 30	Scapolite Pyroxene		Clarendon Twp. Quebec
CA 63A	Scapolite Apatite Fluorite Uranothorite Allanite		Grand Calumet Twp. Quebec

TABLE 1 CONT'D

SAMPLE	MINERAL ASSEMBLAGE	COMMENTS ON POWDER	LOCALITY
Q 87	Scapolite Pyroxene Sphene Fluorite Calcite		Huddersfield Twp. Quebec
Q 26	Scapolite Quartz Sphene		Clapham Twp. Quebec
Q 13A	Scapolite Augite Phlogopite Calcite		Huddersfield Twp. Quebec
ON 27	Scapolite Pyroxene Graphite Calcite		Olmsteadville N.Y.
Q 85	Scapolite Calcite Amphibole Diopside	1% feldspar slight fibrous alteration	Huddersfield Twp. Quebec
ON 47	Single crystal of scapolite with inclusions of pyroxene		Slyudyanka Siberia, U.S.S.R. R.O.M. M18778

Note: All samples except ON 70 were provided by D.M. Shaw.

from An_0 to An_{100} in 10 mole per cent intervals, and have been studied in detail by J.V. Smith (1966)

Determination and Discussion of Chemical Properties of Scapolite Standards.

Seven of the thirteen scapolite samples used as standards were analyzed by J. Muysson, McMaster University; Table 2 presents the chemical analyses. Sample GL had previously been analyzed by J. Muysson. Analyses by C.O. Ingamells, Rock Analysis Laboratory, Pennsylvania State University were available for Q 85, Q 87A, ON 6A and ON 8.

In order to examine the various physical and chemical trends, graphs of physical and chemical variables were plotted against mole per cent meionite. The meionite percentage is given as the following ratio:

$$\frac{Ca + Mg + Fe + Mn + Ti}{Na + K + Ca + Mg + Fe + Mn + Ti}$$

The above relation may be written

$$\frac{Ca^*}{Ca^* + Na^*}$$

where $Ca^* = Ca + Mg + Fe + Mn + Ti$

$$Na^* = Na + K$$

This function arises from the general formula established by Shaw (1960): $W_4Z_{12}O_{24}R$

TABLE 2
SCAPOLITE ANALYSES

21.

Wt%	ON 70	ON 3B	Q 30	CA 63A	Analyst's Notes
SiO ₂	53.06	52.20	52.50	52.04	
TiO ₂	0.00	0.02	0.00	0.01	
Al ₂ O ₃	23.20	23.74	23.45	22.55*	*Could be low F interferes
Fe ₂ O ₃	0.19	0.07	0.10	0.10	
MnO	0.02	0.01	0.01	0.01	
MgO	0.02	0.15	0.34	0.09	
CaO	9.88	10.43	10.45	11.05	
Na ₂ O	7.65	7.45	7.27	7.20	
K ₂ O	0.95	0.58	0.86	0.93	
P ₂ O ₅	0.00	0.03	0.00	0.00	
H ₂ O ⁺	0.08	0.22	0.20	0.14	
H ₂ O ⁻	0.03	0.01	0.09	0.00	
CO ₂	2.18	2.53	1.77	--	
SrO	0.07	0.21	0.10	0.32	
BaO	0.00	0.00	0.00	0.00	
SO ₃	1.10	1.1**	0.88	0.6**	**loss of precision
Cl	1.90	1.5**	2.00	1.6**	
F	0.00	0.00	0.00	0.76	
Sum	100.33	100.25	100.02	97.40	
Less	0.43	0.34	0.45	0.68	O=Cl,F
Total	99.90	99.9	99.57	96.70	

TABLE 2 CONT'D

22.

Wt. %	Q 26	Q 13A	ON 27	ON 47
SiO ₂	51.67	50.14	48.98	44.05
TiO ₂	0.00	0.00	0.02	0.01
Al ₂ O ₃	23.98	24.57	25.51	28.67
Fe ₂ O ₃	0.16	0.03	0.25	0.08
MnO	0.01	0.00	0.00	0.01
MgO	0.02	0.06	0.08	0.07
CaO	11.30	12.56	14.11	18.65
Na ₂ O	6.30	5.70	4.63	2.55
K ₂ O	1.07	0.93	1.27	0.24
P ₂ O ₅	0.01	0.01	0.01	0.00
H ₂ O ⁺	0.11	0.07	--	0.26
H ₂ O ⁻	0.03	0.22	0--	0.13
CO ₂	2.55	3.04	--	3.20
SrO	0.20	0.25	0.14	0.19
BaO	0.00	0.00	0.00	0.00
SO ₃	1.08	1.16	--	1.63
Cl	1.75	1.52	--	0.03
F	0.00	0.00	--	0.00
Sum	100.24	100.26	(95.00)	99.77
Less	0.39	0.34		0.01 0 = Cl, F
Total	99.85	99.92		99.76

TABLE 2 CONT'D

Wt. %	ON 8	G.L.	ON 6A	Q 87	Q 85
SiO ₂	57.89	55.44	54.73	52.10	47.17
TiO ₂	0.01	Trace	0.01	0.02	0.03
Al ₂ O ₃	21.62	22.89	22.85	23.79	26.29
Fe ₂ O ₃	0.07	0.00	0.08	0.23	0.15
MnO	0.01	0.00	0.00	Trace	0.01
MgO	0.03	0.30	0.03	0.18	1.00
CaO	4.81	7.72	8.29	11.13	14.31
Na ₂ O	10.50	9.36	8.55	6.86	3.82
K ₂ O	1.16	0.22	1.08	0.87	1.01
P ₂ O ₅	--	0.05	--	--	--
H ₂ O ⁺	0.44	0.22	0.13	0.07	0.93
H ₂ O ⁻	0.06	0.03	0.00	0.10	0.50
CO ₂	1.11	1.85	1.69	2.14	2.66
SO ₃	0.03	0.18	0.39	0.80	1.42
Cl	2.96	2.30	2.19	1.85	0.56
F	0.00	0.00	0.00	0.11	0.04
Sum	100.70	100.37	100.02	100.25	99.90
Less	0.67	0.48	0.49	0.46	0.14 O=Cl, F
Total	100.03	99.89	99.53	99.79	99.76

Note: Total Fe as Fe₂O₃
 --indicates no determination

TABLE 3

Gram Atom Values and Corresponding Mole Per Cent Meionite
(Si + Al = 12000)

Sample	ON 70	ON 3B	Q 30	CA 63A
Element				
Si	7919	7812	7861	7943
Ti	0.0	2.2	0.0	1.1
Al	4081	4188	4139	4057
Fe	21.3	7.8	11.2	11.4
Mn	2.5	1.2	1.2	1.2
Mg	4.4	33.4	75.8	20.4
Ca	1579	1672	1677	1807
Na	2213	2162	2111	2131
K	180.8	110.7	164.2	181.0
P	0	3.8	0	0
H	79.6	219.6	199.8	142.5
C	444	516.9	361.8	
Sr	6	18.2	8.6	68.7
Ba	0	0	0	0
S	123.2	123.5	98.8	68.7
Cl	480.5	380.4	507.5	413.9
F	0.0	0.0	0.0	366.8
Na*	2395	2273	2275	2312
Ca*	1608	1717	1765	1842
AN	1047	1021	968	850
W	4003	3990	4040	4153
% Me	40.18	43.04	43.69	44.34

TABLE 3 CONT'D

Sample	Q 26	Q 13A	ON 27	ON 47
Element				
Si	7757	7607	7436	6791
Ti	0.0	0.0	2.2	1.1
Al	4243	4393	4564	5209
Fe	18.0	3.4	28.5	9.2
Mn	1.2	0.0	0.0	1.3
Mg	4.4	13.5	18.1	16.0
Ca	1818	2042	2295	3080
Na	1834	1677	1363	762
K	205	179.9	246	47
P	1.2	1.2	1.2	0.0
H	1110.1	70.8	--	267.3
C	522.6	630	--	673.5
Sr	17.4	21.9	12.3	16.9
Ba	0.0	0.0	0.0	0.0
S	121.6	132.0	--	188.5
Cl	445.2	391.0	--	7.8
F	0.0	0.0	--	0.0
Na*	2039	1857	1609	809
Ca*	1841	2059	2344	3108
AN	1090	1153	--	869.9
W	3880	3915	3953	3918
% Me	47.46	52.58	59.30	79.34

TABLE 3 CONT'D

Sample	ON 8	GL	ON 6A	Q 87	Q 85
Element					
Si	8334	8054	8046	7803	7243
Ti	1	--	1	2	4
Al	3666	3946	3954	4197	4757
Fe	8	--	9	26	18
Mn	1	--	--	--	1
Mg	7	55	7	41	231
Ca	744	1234	1309	1786	2362
Na	2934	2639	2435	1995	1137
K	214	41	203	167	198
P	--	--	--	--	--
H	422	214	127	70	950
C	218	371	339	438	558
Sr	--	--	--	--	--
Ba	--	--	--	--	--
S	3	20	43	90	163
Cl	721	589	544	471	146
F	--	--	--	52	19
Na*	3148	2680	2638	2162	1335
Ca*	753	1289	1322	1829	2598
AN	942	980	927	1051	886
W	3901	3969	3960	3991	3933
% Me	19.4	32.5	33.5	46.2	66.2

Na* = Na + K, Ca* = Ca + Ti + Mg + Mn, AN = C + F + Cl + S
W = Ca* + Na*

where $W = Ca^* \text{ and } Na^*$

$$Z = Si + Al$$

$R = \text{volatile components, } Cl, CO_3, SO_3^{**}$

Each chemical analysis was converted to gram atom values on the basis of $Si + Al = 12,000$. The data so obtained are tabulated in Table 3.

From a study of Tables 2 and 3 it appears that there is no regular relationship between mole per cent meionite and the elements Ti, Fe, Mn, Mg, P, H, F, K, Ba, Sr, F. In Figures 2 to 8, Wt. % Cl , SO_3 , CO_2 , Na_2O , CaO , Al_2O_3 and SiO_2 have been plotted versus mole per cent meionite. The relationship between each component and mole per cent meionite appears to be linear, represented by the equation $Wt \% \text{ component} = \alpha + \beta \text{ mole \% Me}$. For each chemical component α and β have been determined and the values of these at 95% confidence limits. The values so determined have been presented with the graphs of the above mentioned variables. Those Wt% values having analyst's notes indicating lack of precision have not been considered in the linear regression analysis. As expected Wt% Na_2O , CaO , Al_2O_3 , SiO_2 versus mole per cent meionite have high correlation coefficients.

** Sulphur is considered as occurring in the form $SO_3^{=}$ as indicated by wavelength studies, discussed in a later section.

FIGURE 2

Mole % Meionite vs Weight % Cl

Linear Regression Equation

$$\text{Wt. \% Cl} = 3.9839 - 0.0492 \text{ Mole \% Me}$$

α β

Confidence Limits at 95% Level

$$3.6941 < \alpha < 4.2737$$

$$-0.0552 < \beta < -0.0433$$

Correlation Coefficient = -0.989

Analyst's Notes:

ON 3 Loss of precision in analysis.

CA 63A

"

ON 27 not determined

(These samples not included in regression analysis)

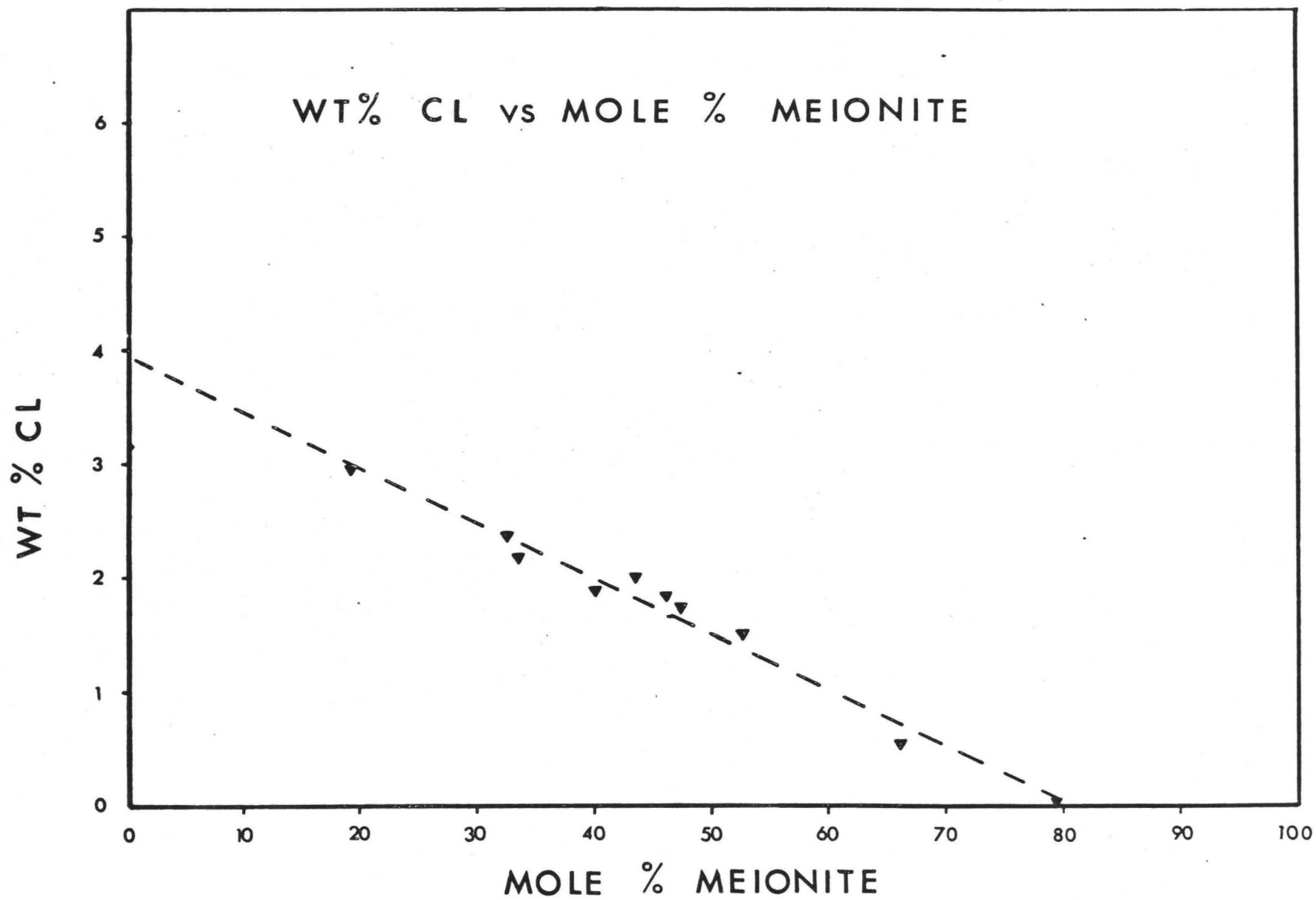


FIGURE 2

FIGURE 3

Mole % Meionite vs Weight % SO_3

Linear Regression Equation

$$\text{Wt \% SO}_3 = -0.4335 + 0.0282 \text{ Mole \% Me}$$

α β

Confidence Limits at 95% Level

$$-0.8933 < \alpha < 0.0263$$

$$0.0188 < \beta < 0.0376$$

Correlation Coefficient = 0.926

Analyst's Notes:

ON 27 not determined

CA 63A loss of precision

ON 3B "

(These samples not included in linear regression analysis.)

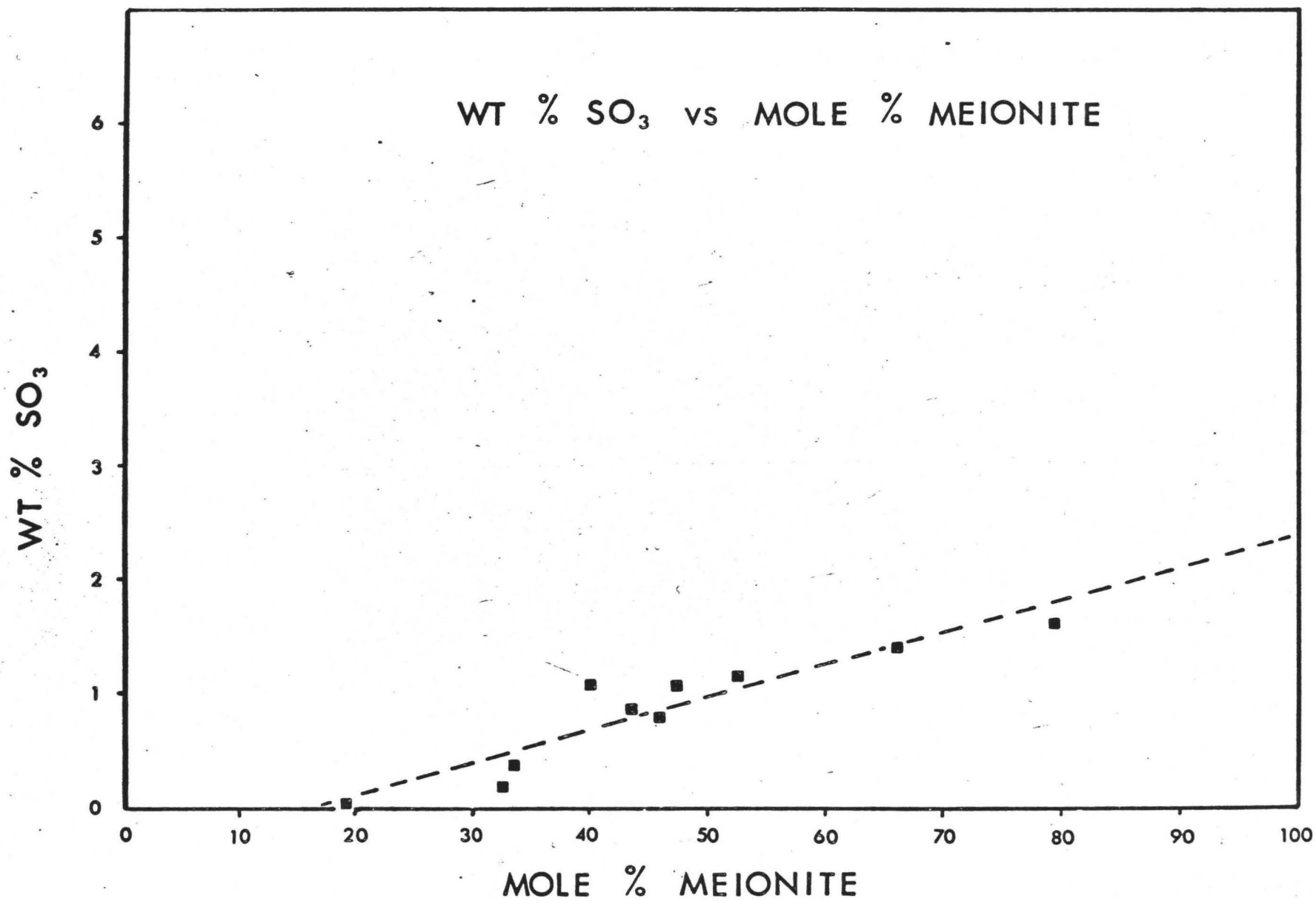


FIGURE 3

FIGURE 4

Mole % Meionite vs Weight % CO₂

Linear Regression Equation

$$\text{Wt. \% CO}_2 = 0.7201 + 0.0334 \text{ Mole \% Me}$$

α β

Confidence Limits at 95% Level

$$0.0457 < \alpha < 1.3945$$

$$0.0194 < \beta < 0.0473$$

Correlation Coefficient = 0.875

Analyst's Notes:

CA 63A not determined

ON 27

"

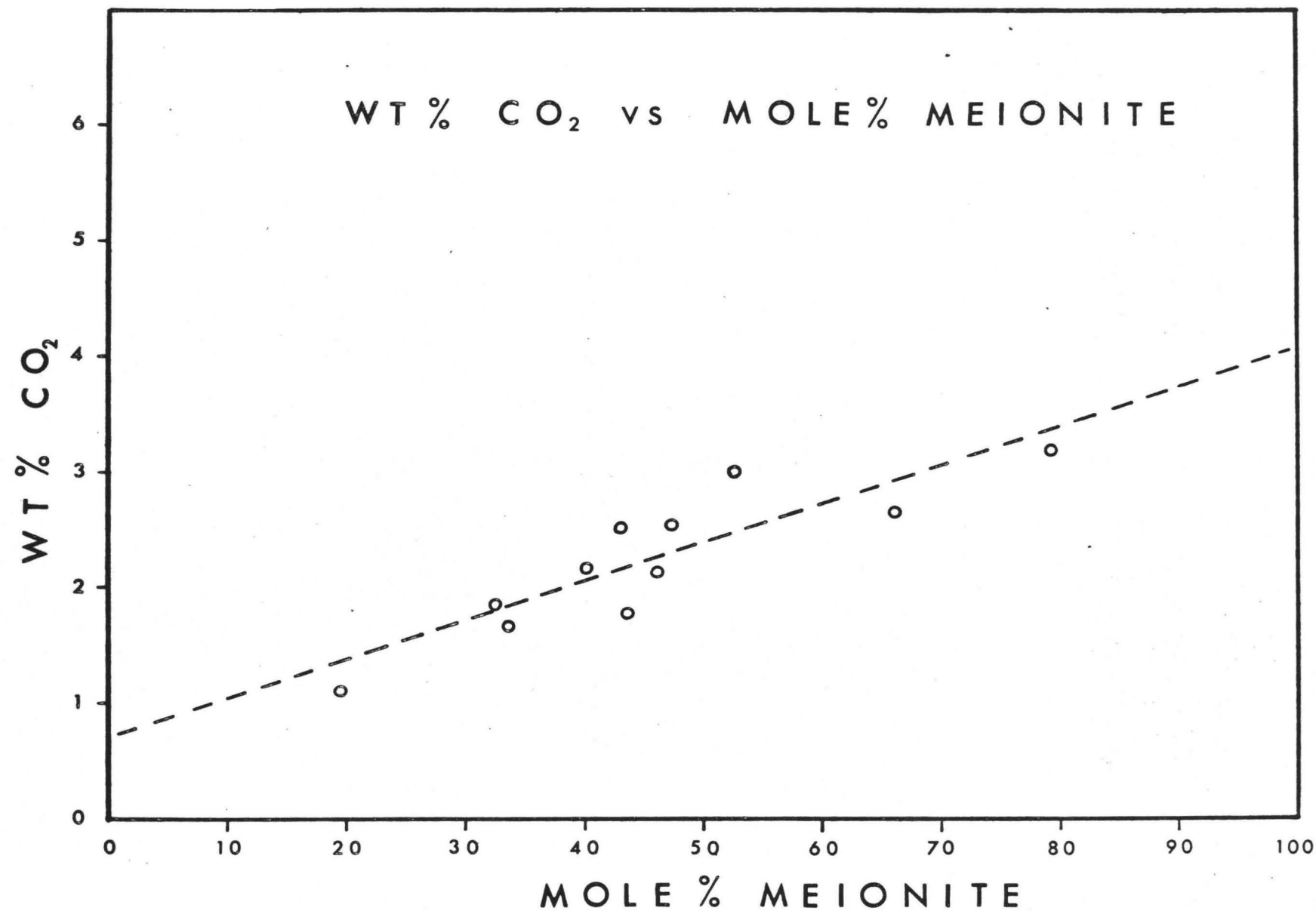


FIGURE 4

FIGURE 5

Mole % Meionite vs Weight % Na₂O

Linear Regression Equation

$$\text{Wt. \% Na}_2\text{O} = 13.3840 - 0.1418 \text{ Mole \% Me}$$

α β

Confidence Limits at 95% Level'

$$12.8063 < \alpha < 13.9617$$

$$-0.1536 < \beta < -0.1300$$

$$\text{Correlation Coefficient} = -0.992$$

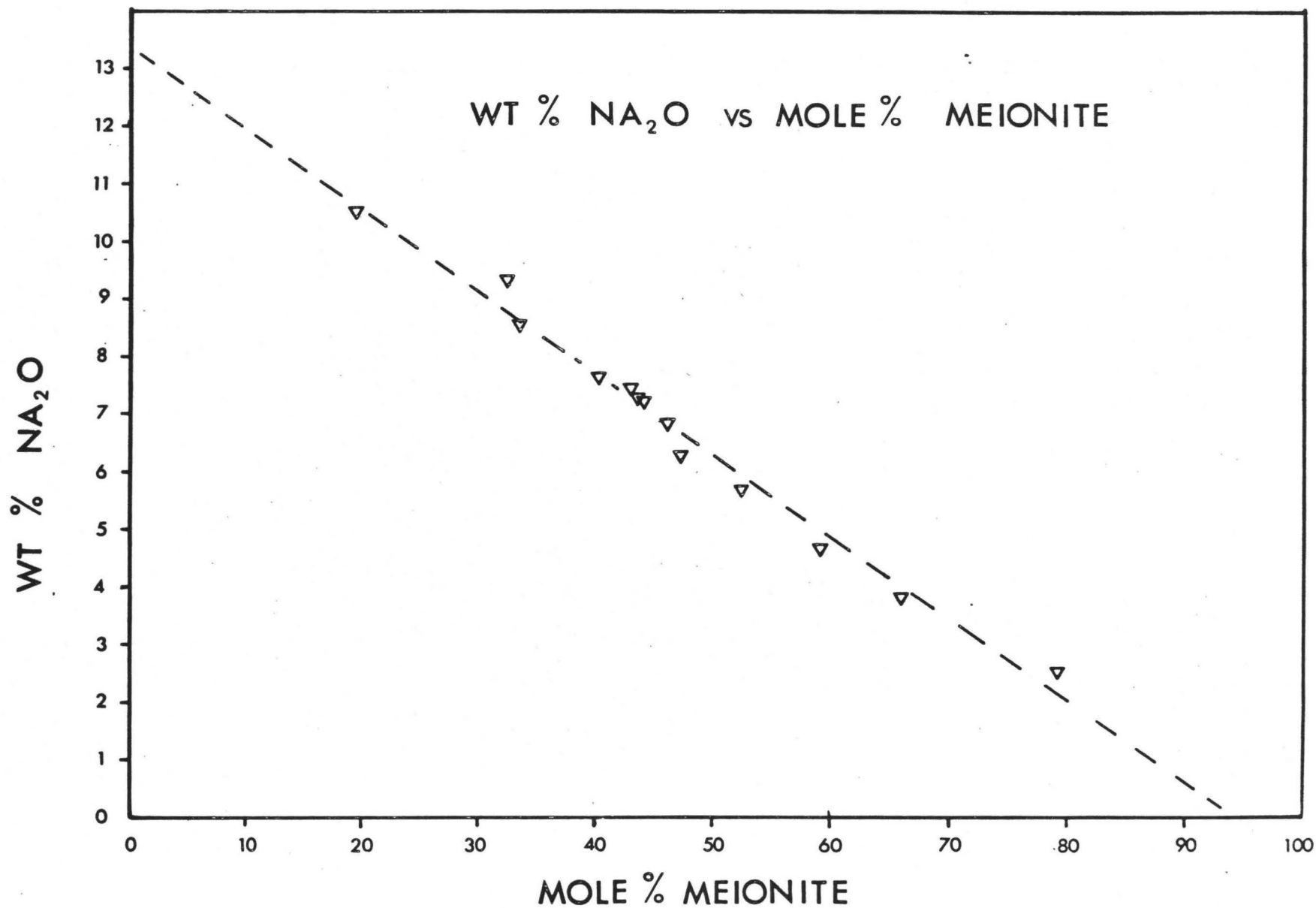


FIGURE 5

FIGURE 6

Mole % Me vs Weight % CaO

Linear Regression Equation

$$\text{Wt. \% CaO} = 0.5249 + 0.2295 \text{ Mole \% Me}$$

α β

Condidence Limits at 95% Level

$$0.2116 < \alpha < 0.8382$$

$$0.2228 < \beta < 0.2361$$

Correlation Coefficient = 0.999

Note: Q 85 not included in linear regression analysis.

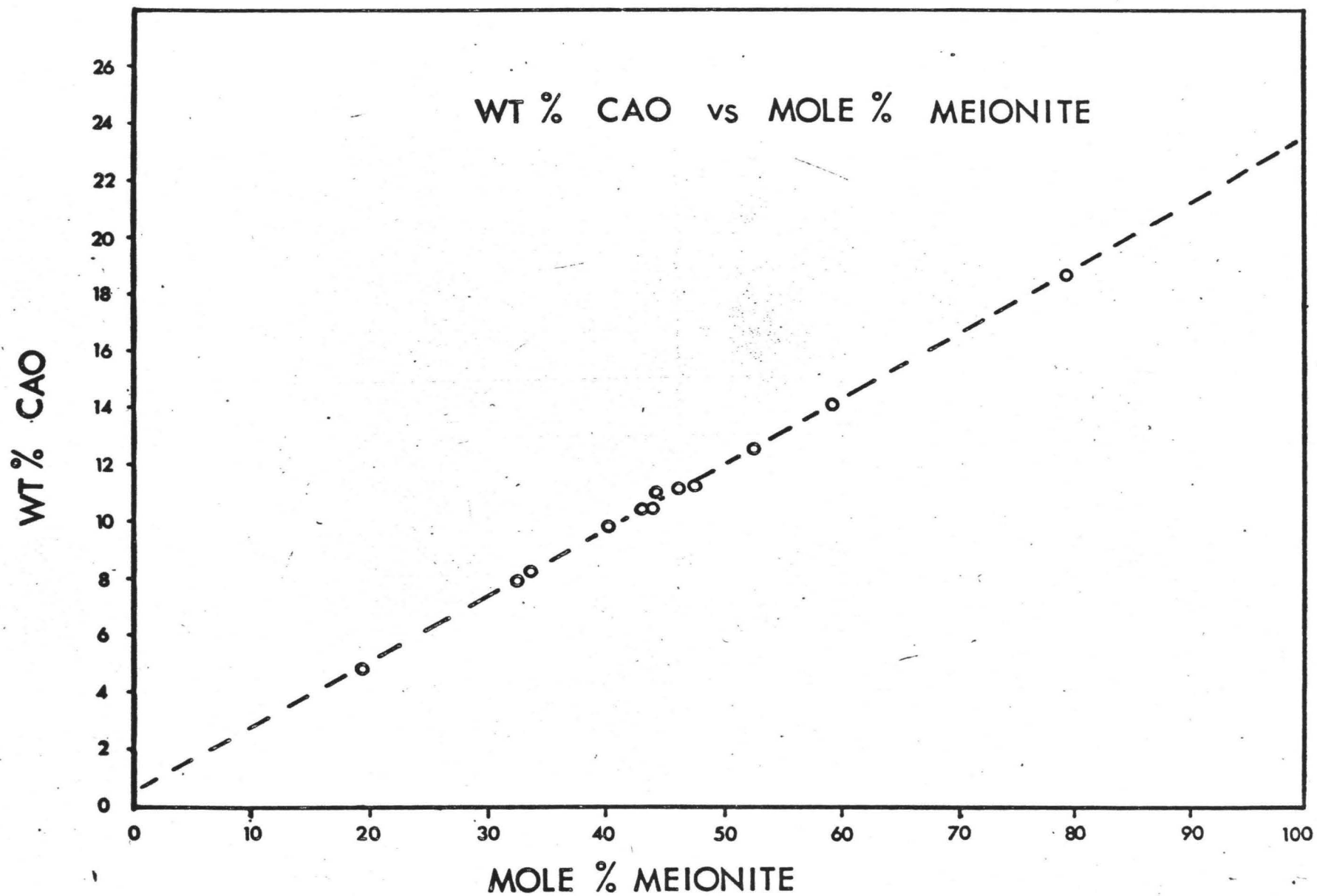


FIGURE 6

FIGURE 7

Mole % Me vs Weight % Al_2O_3

Linear Regression Equation

$$\text{Wt. \% Al}_2\text{O}_3 = 18.8741 + 0.1139 \text{ Mole \% Me}$$

α β

Confidence Limits at 95% Level

$$18.0494 < \alpha < 19.6988$$

$$0.0972 < \beta < 0.1306$$

Correlation Coefficient = 0.979

Analyst's Notes:

CA 63A Could be low, F interferes.

(This sample not included in linear regression analysis).

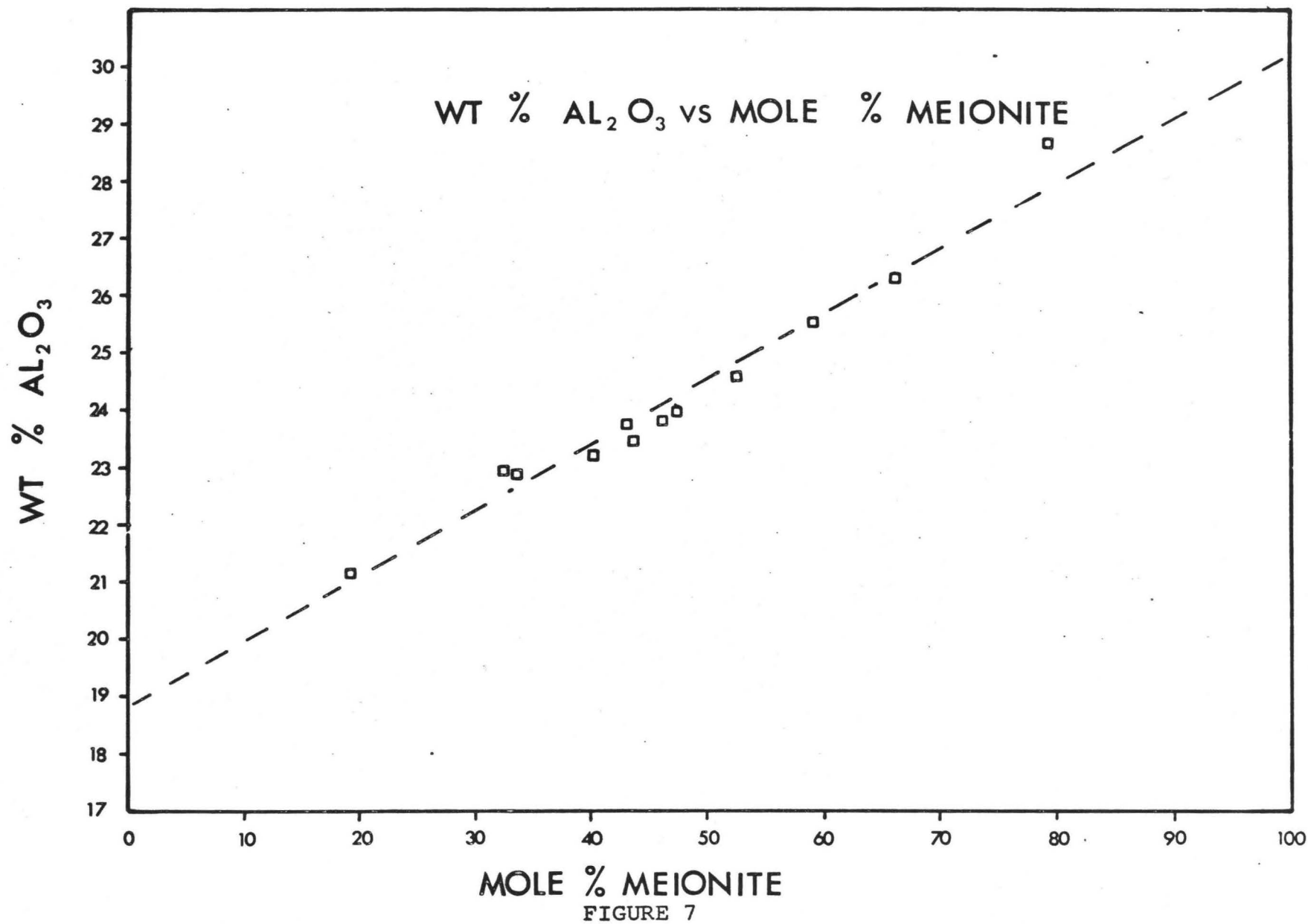


FIGURE 8

Mole % Me vs Weight % SiO_2

Linear Regression Equation

$$\text{Wt. \% SiO}_2 = 62.4769 - 0.2311 \text{ Mole \% Me}$$

α β

Confidence limits at 95% Level

$$62.0662 < \alpha < 62.8876$$

$$-0.2395 < \beta < -0.2227$$

Correlation Coefficient = -0.999

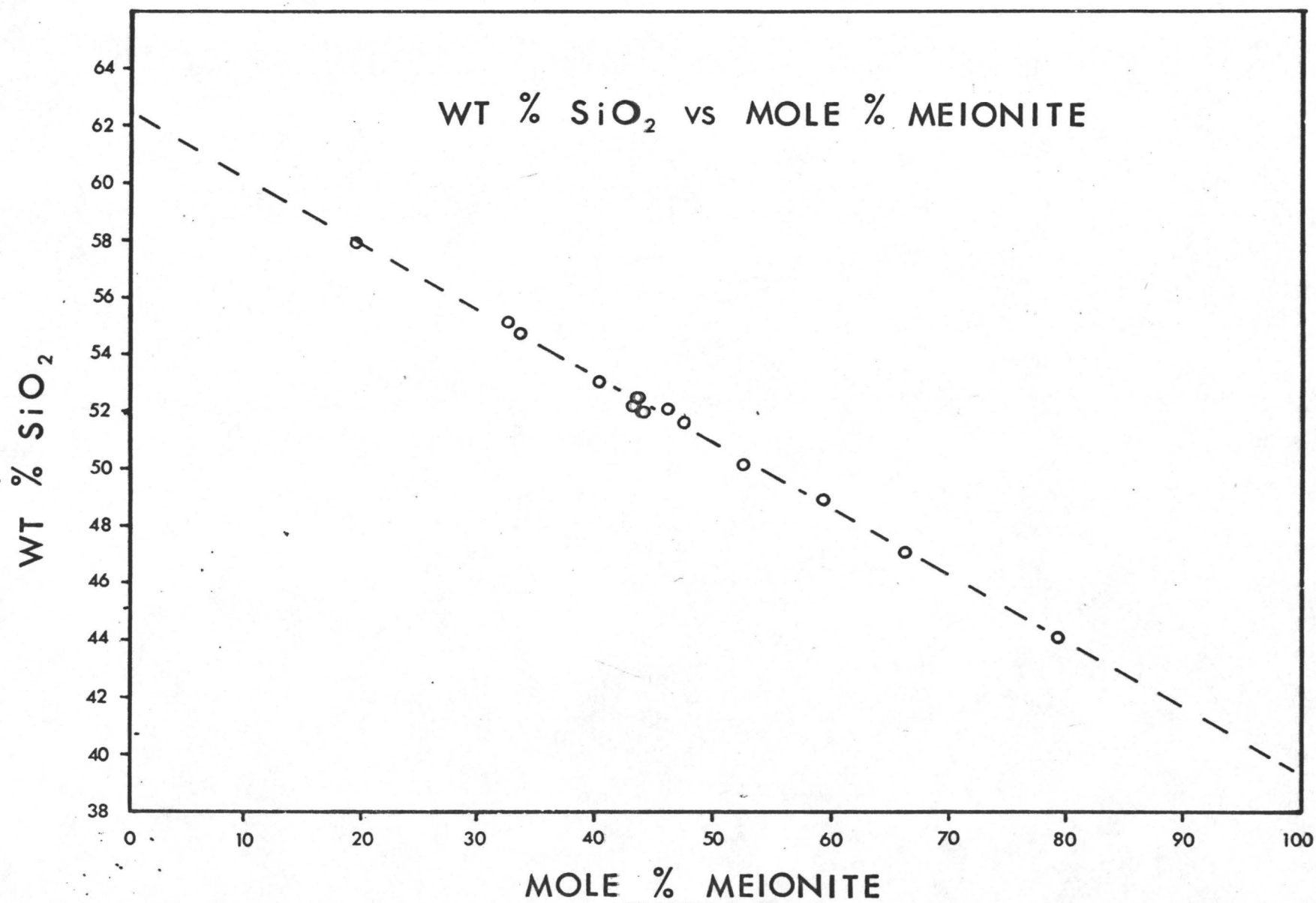


FIGURE 8

The correlation coefficient for weight per cent CaO versus mole per cent meionite equals 0.999. This however excludes the point Q 85 which deviates from the linear regression equation by more than 6 mole per cent meionite and 1 weight per cent CaO. It was noted that Q 85 contained 1 per feldspar of unknown composition. The probe results (see later) indicate that scapolite is more Ca-rich than the coexisting plagioclase; this may account for the deviation from the determined linear curve. In view of the above and its extreme departure from the linear trend this point was omitted from the linear regression analysis.

Considering the volatiles Cl, CO₂, and SO₃, the following points are notable: Cl has a correlation coefficient of -0.989 indicating that mole per cent meionite is an excellent indicator of weight per cent Cl. It is interesting that weight per cent Cl equals 0 at 80.92 mole per cent meionite, and the significance of this will be considered in detail in a following section. The correlation coefficient for weight per cent SO₃ versus mole per cent meionite is equal to 0.926 indicating that mole per cent meionite is also an excellent indicator of

weight per cent SO_3 . Note that weight per cent SO_3 is equal to 0 at 15.36 mole per cent meionite. The correlation coefficient of .875 indicates that mole per cent meionite is a fair indicator of weight per cent CO_2 . Solving the linear regression equation at 0 mole per cent meionite, weight per cent CO_2 equals 0.72. However it is notable that weight per cent CO_2 equal to 0.05 falls within the 95% confidence limits. Therefore although there is an indication that marialite may contain CO_2 such a conclusion would require further investigation.

Studying the relationships among the volatile components it is observed that CO_2 and SO_3 increase regularly with increasing mole per cent meionite. (Figures 3 and 4). This increase is correlated directly with a decrease in Cl. (Figure 2).

Tschermak*(1883) illustrated that the scapolite system could be represented as a solid solution series of the end members meionite, $\text{Ca}_4\text{Al}_6\text{Si}_6\text{O}_{25}$ and marialite, $\text{Na}_4\text{Al}_3\text{Si}_9\text{O}_{24}\text{Cl}$. Brauns*(1914) continuing the work of Tschermak observed that SO_3 varied sympathetically with CaO . Shortly after, Borgstrom*(1915) recognized that

* See Shaw (1960)

CO₂ was an essential constituent. Therefore for the regular relationships observed agree with earlier findings.

End Member Formulae.

The linear regression curves in previous sections have illustrated that there is a simple relation among the components of scapolite and the mole per cent meionite. Therefore it is suitable that a general formula be derived for scapolite.

The weight percentages of the components determined by extrapolation at the 0, and 100 mole per cent meionite points (Table 4) have been used to determine the gram atom values for major elements in scapolite (Table 5). The Wt % CO₂ was not utilized in this manner for reasons previously described and will only be considered qualitatively. Using the values from Table 5 a general formula may be developed. The formula developed follows that of D.M. Shaw (1960).



W is principally Ca and Na

Z represents Si and Al

R represents Cl⁻, SO₃, CO₃⁼

TABLE 4
Solution of Linear Regression Equations for 0 and 100 per cent
Values

Me %	0	100
Wt % Component		
	(Wt % Cl = 0, mole % Me = 80.92)	
Cl	3.98	-0.94*
	(Wt % SO ₃ = 0, mole % Me = 15.36)	
SO ₃	-0.43*	2.39
CO ₂	0.72**	4.06**
CaO	0.52***	23.47
Na ₂ O	13.38	-0.80***
Al ₂ O ₃	18.87	30.26
SiO ₂	62.48	39.37
Total	99.95	99.55
(excluding negative values)		

* All negative values ignored.

** These values have not been considered in determination of end member formulae.

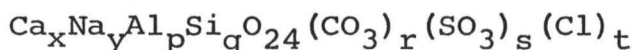
*** When considering end member formulae these values are assumed to be 0. This follows from the definition of mole per cent meionite.

TABLE 5

Conversion from Weight per cent to Gram Atom Values
(Si + Al = 12000)

Mole % Meionite	0	100
Wt % Component		
SiO ₂	62.48	39.37
Al ₂ O ₃	18.87	30.26
CaO	0	23.47
Na ₂ O	13.38	0
SO ₃	0	2.39
Cl	3.98	0
Ionic Proportions (Gram Atoms)		
Si	8850	6296
Al	3150	5704
Ca	0	4022
Na	3676	0
S	0	287
Cl	955	0

The ideal formula may thus be expressed in the form:



where x and y define the mole per cent meionite as

$$\frac{100x}{x + y}$$

and p, q, r, s, and t are functions of x and y.

Utilizing the data in Table 5, assuming $\text{Si} + \text{Al} = 12$ and $x + y = 4$ a formula describing scapolite compositional variation may be developed, where:

$$p = 3 + \frac{3x}{x + y}$$

$$q = 9 - \frac{3x}{x + y}$$

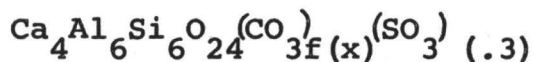
$$r = f(x, y) \text{ increasing as } \frac{x}{x + y} \text{ approaches } 1$$

$$s = -0.05444 + 0.3544 \frac{x}{x + y}$$

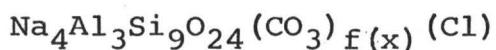
$$t = 1 - 1.2358 \frac{x}{x + y}$$

All negative values are ignored.

Substituting $x = 4$ in the above equations the formula for meionite is:



If $y = 4$ the formula for marialite is:



It has been demonstrated that the compositional variation of scapolite may be defined by two end members only. The sodic end member, marialite is rich in chlorine, and the calcic end member, meionite is rich in carbonate and sulphite ions.

Although meionite and marialite do not appear to be stable in nature nevertheless the end member formulae for meionite (Me_{100}) and marialite (Me_0) serve as useful reference formulae.

Determination and Discussion of Physical Properties of Scapolite Standards.

Specific Gravity: The specific gravity of twelve of the thirteen standards was determined. The specific gravity of ON 8 was not determined due to lack of sample. Numerous small samples of the particular scapolite studied were placed in tetrabromethane (S.G. = 2.95, $T = 25^\circ\text{C}$). To this were added small amounts of dimethylformamide chosen because of its low specific gravity (S.G. = 0.94, $T = 25^\circ\text{C}$). The latter liquid was added to the tetrabromethane until scapolite particles became suspended.

The liquid was assumed to have the same specific gravity as the scapolite particles. A 10 ml. pycnometer was then used to determine the specific gravity of the liquids. Before use the pycnometer bottle was thoroughly washed with acetone and dried. When filling, the bottle was wrapped in absorbent tissue to prevent any of the liquid coming in contact with the outside of the bottle. The bottle stopper was then inserted; the pycnometer was then cleaned with absorbent tissue dampened by acetone. Acetone was not used directly on the bottle since this produced a notable cooling effect accompanied by a drop in the level of the liquid in the capillary tube of the stopper. The bottle and contents were weighed two minutes after the time of cleaning and thereafter at five two minute intervals. A graph of weight versus time was then plotted, and extrapolated to zero time.

All weights were determined to five places after the decimal point. Temperature during the determination was recorded and was noted to be $24^{\circ}\text{C} \pm 2^{\circ}\text{C}$. Through a consideration of reproducibility and specific gravity determinations of minerals of constant specific gravity it is estimated that this method is accurate to $\pm .005$ units. Table 6 lists the results of the determinations.

TABLE 6
Specific Gravity Determinations

Specimen	% Me	S.G. D.R.H.	S.G. J.N.W.*
ON 8	19.4	--	2.619
GL	32.5	2.626	
ON 6A	33.5	2.633	2.660
ON 70	40.18	2.667	
ON 3B	43.04	2.656	
Q 30	43.69	2.669	
CA 63A	44.34	2.629	
Q 87	46.2	2.681	2.689
Q 26	47.46	2.674	
Q 13A	52.58	2.672	
ON 27	59.30	2.694	
Q 85	66.2	2.693	2.705
ON 47	79.34	2.733	

*by J.N. Weber,
in Shaw (1960)

Specific gravity determinations cover a range between 2.619 and 2.733 (Figure 9). Scatter is however quite great so that use of specific gravity as a determinative technique is limited. This is in agreement with the observations of Shaw (1960). The general tendency noted is an increase in specific gravity with increasing mole per cent meionite. It is thought that much of the scatter might be due to lack of sensitivity of the method used rather than actual variation of scapolite specific gravity.

FIGURE 9

Specific Gravity vs Mole % Meionite

Note: darkened points represent those
values determined by J.N. Weber.

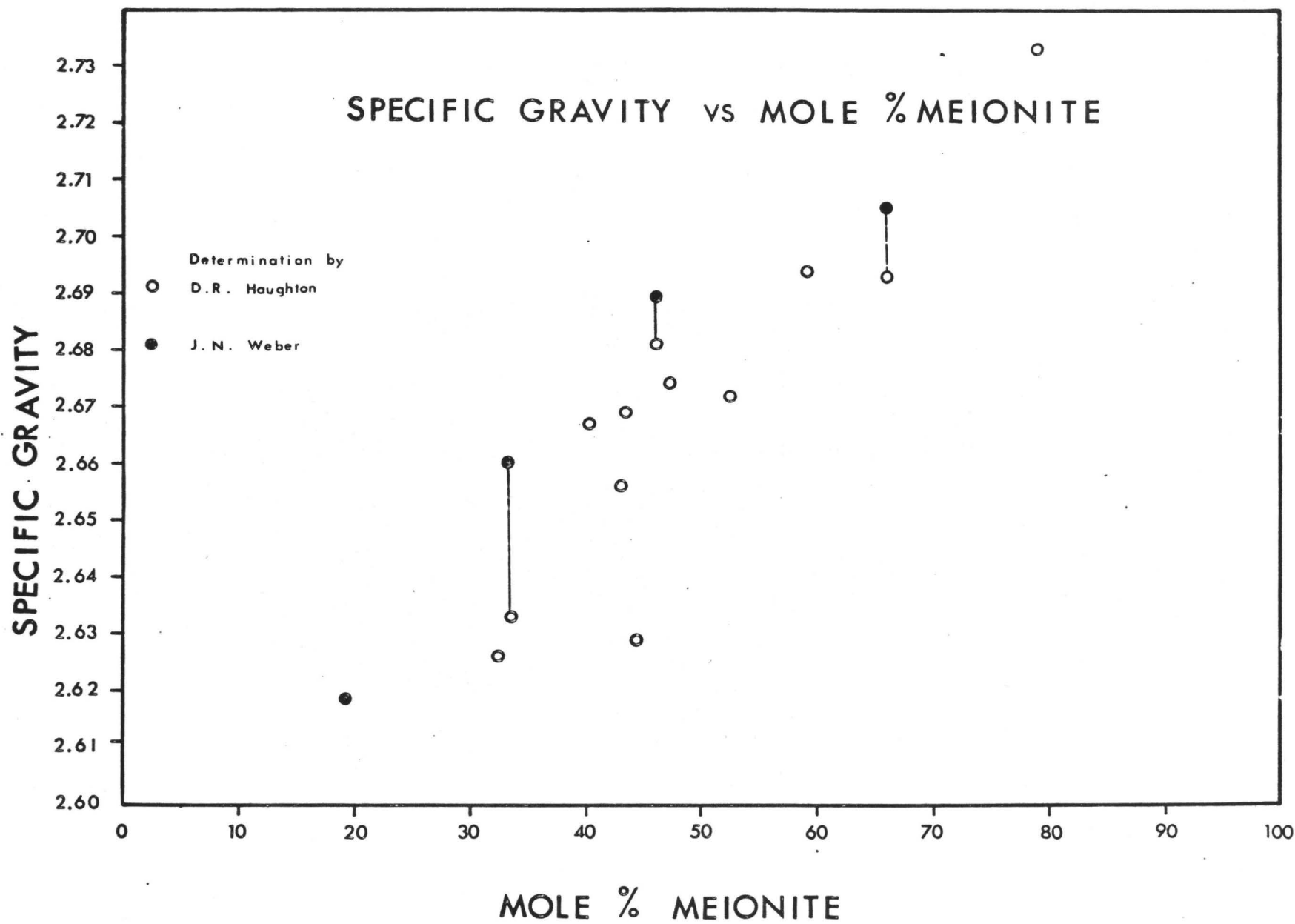


FIGURE 9

Refractive Index: Refractive indices were determined through the use of a new set of Cargille index of refraction liquids. Sodium light was used as the monochromatic light source. Under ideal conditions with media available in steps of 0.002 and calibrated to an accuracy of ± 0.0002 an accuracy of ± 0.001 is possible. Table 7 presents the information obtained. It may be noted that my determinations are in excellent agreement with those done by D.M. Shaw (1960).

TABLE 7
Optical Parameters

Sample	n_o D.R.H.	n_o D.M.S.	n_e D.R.H.	n_e D.M.S.	dn D.R.H.	$\frac{n_o+n_e}{2}$ D.R.H.
ON 8	1.546	1.549	1.542	1.541	0.004	1.544
GL	1.562		1.546		0.016	1.554
ON 6A	1.561	1.560	1.546	1.547	0.015	1.5535
ON 70	1.566		1.550		0.016	1.558
ON 3B	1.564	1.566	1.548	1.550	0.016	1.556
Q 30	1.565	1.567	1.548	1.549	0.017	1.5565
CA 63A	1.559	1.565	1.545	1.548	0.014	1.552
Q 87	1.566	1.568	1.550	1.550	0.016	1.558
Q 26	1.570	1.572	1.552	1.552	0.018	1.561
Q 13A	1.570	1.571	1.550	1.551	0.020	1.5645
ON 27	1.579	1.577	1.550	1.550	0.029	1.5645
Q 85	1.581	1.581	1.558	1.557	0.023	1.5695
ON 47	1.592	1.592	1.561	1.560	0.031	1.5765

The optical parameters determined have been plotted in Figure 10. Any scatter greater than 0.001 may be a result of substitution of ions such as Mg^{2+} , Fe^{2+} , Fe^{3+} , Mn^{2+} , Ti^{2+} and K^{+} in the scapolite structure. The distortions in the structure caused by incorporation of these ions may be reflected by slight variations in refractive index. The point representing CA 63A deviates from the dashed lines (n_o and n_e versus mole % meionite) by over 10% meionite. It is unlikely that errors are of such magnitude. If birefringence is plotted against mole per cent meionite, one finds that a small scatter of points is evident. It is noted that birefringence, mean refractive index and refractive index generally show a regular increase with increasing mole per cent meionite. It is also notable that n_e approaches n_o as mole per cent meionite decreases to zero.

Lattice Parameter Determination: The unit cell dimensions were obtained from measurements taken from Debye-Scherrer (114.6 diameter camera) films. Measurements were also obtained from charts obtained from a Philips Geiger-counter x-ray goniometer unit. Quartz was used as an internal standard when using the charts. Accuracy in,

FIGURE 10

Optical Properties of Scapolite

dn = Birefringence

RI = Refractive Index

$$\frac{n_o + n_e}{2} = \text{Mean Refractive Index}$$

*

The equation for the Mean Refractive Index is:

$$\frac{n_o + n_e}{2} = 1.5347 + 0.000507 (\text{Me}\%)$$

Note: -* in Shaw (1960)

--Darkened points in RI indicate those values determined by D.M. Shaw (1960)

OPTICAL PROPERTIES OF SCAPOLITE

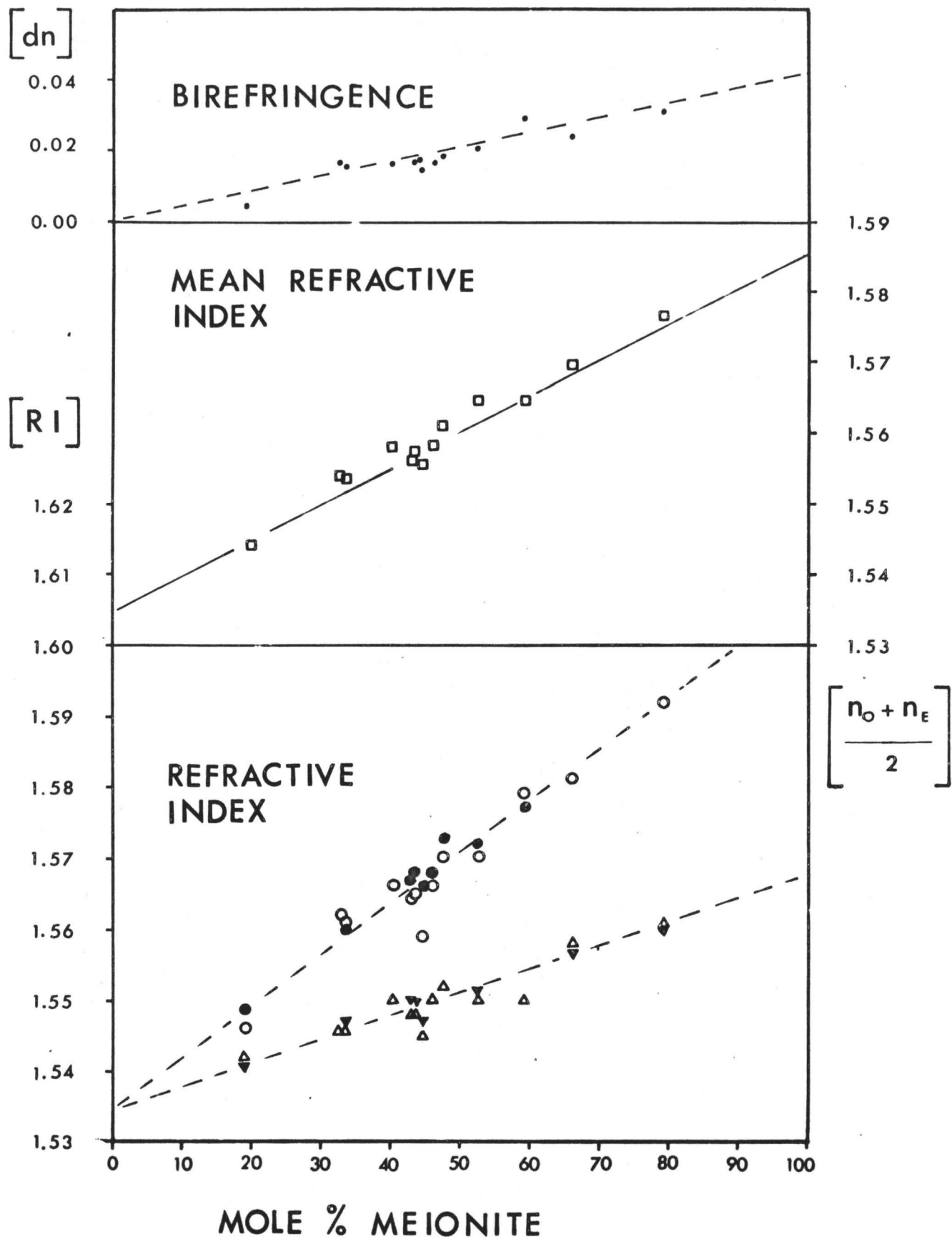


FIGURE 10

measurement was ± 0.005 degrees 2θ . In both methods $\text{CuK}\alpha$ radiation was used. The data obtained were processed in a linear regression program contributed by B. Robertson, McMaster University. The program adjusted the values of the reciprocal cell constants to fit observed Debye-Scherrer lines or Geiger chart values, by generalizing Gaussian least squares. Any peaks which were vague or extremely broad were not recorded. Thus in many cases only a few excellent peaks were used. Calculated powder patterns (Papike 1964) were used to index the various reflections. The Miller indices, θ (observed) and the lattice parameters determined are listed in Table 8. Cell parameters were determined for eight of the thirteen probe standards.

Figure 11 illustrates the results of this study, as obtained from Table 8. Four of the values plotted in Figure 11 were obtained from Papike (1964). The remaining eight were determined with the use of standard x-ray equipment, previously described. Generally the data show agreement with data of Papike (1964). As indicated by Papike the cell volume may be used to determine composition of scapolite.

TABLE 8Axial Parameters hkl and Respective θ Values

Sample	hkl	θ	a	c	a^2c	Method
ON 8	Data from J.J. Papike		12.060	7.577	1102.03	D.S.*
ON 6A	"		12.075	7.580	1105.21	D.S.
ON 70	143 004 352 710 163 543 235 822 563	23.737 24.050 25.0935 26.865 29.640 30.670 33.935 34.398 35.794	12.068	7.577	1103.49	D.S.
ON 3B	310 112 231 040 312 004	11.670 12.858 14.580 14.830 16.660 24.013	12.057	7.579	1101.77	C**
Q 30	13,2,5 828 10,1,7 4,14,2 895	78.526 75.454 73.159 71.734 66.96	12.090	7.579	1107.81	D.S.

TABLE 8 CONT'D

Sample	hkl	θ	a	c	a^2c	Method
CA 63A	220	10.405	12.087	7.584	1107.99	C
	310	11.640				
	031	12.530				
	112	12.833				
	231	14.549				
	040	14.765				
	141	16.363				
	312	16.620				
	431	19.585				
	341	19.585				
	143	23.570				
	004	24.003				
Q 87	Data from J.J. Papike		12.095	7.579	1108.72	D.S.
Q 26	310	11.620	12.099	7.579	1109.46	C
	031	12.498				
	112	12.858				
	231	14.548				
	040	14.795				
	141	16.358				
	312	16.640				
	431	19.530				
	341	19.530				
	352	25.074				
	822	34.281				
Q 13A	020	7.310	12.113	7.576	1111.59	C
	310	11.613				
	031	12.493				
	231	14.537				
	040	14.740				
	330	15.665				
	312	16.630				
	431	19.520				
	341	19.520				
	033	21.108				
	143	23.745				
	004	24.013				

TABLE 8 CONT'D

Sample	hkl	θ	a	c	a^2c	Method
ON 27	310	11.583	12.135	7.558	1112.98	C
	031	12.458				
	112	12.865				
	231	14.535				
	040	14.720				
	341	19.480				
	431	19.480				
	323	22.470				
	352	25.030				
	710	26.663				
	163	29.545				
	543	30.583				
	822	34.225				
	282	34.225				
<hr/>						
Q 85	Data from J.J. Papike		12.142	7.756	1116.92	D.S.
<hr/>						
ON 47	211	10.050	12.154	7.575	1118.98	C
	310	11.560				
	112	12.860				
	231	14.593				
	040	14.680				
	141	16.298				
	312	16.600				
	431	19.450				
	341	19.450				
	521	20.863				
	033	21.066				
	323	22.435				
	611	23.500				
	143	23.698				
	004	24.030				
	710	26.705				
	543	30.533				
	235	33.913				
	822	34.123				

* Debye-Scherrer powder camera.

** Chart from a Philips Geiger counter x-ray goniometer unit.

FIGURE 11

Unit Cell Parameters

All lattice dimensions are in Angstrom units.

UNIT CELL PARAMETERS

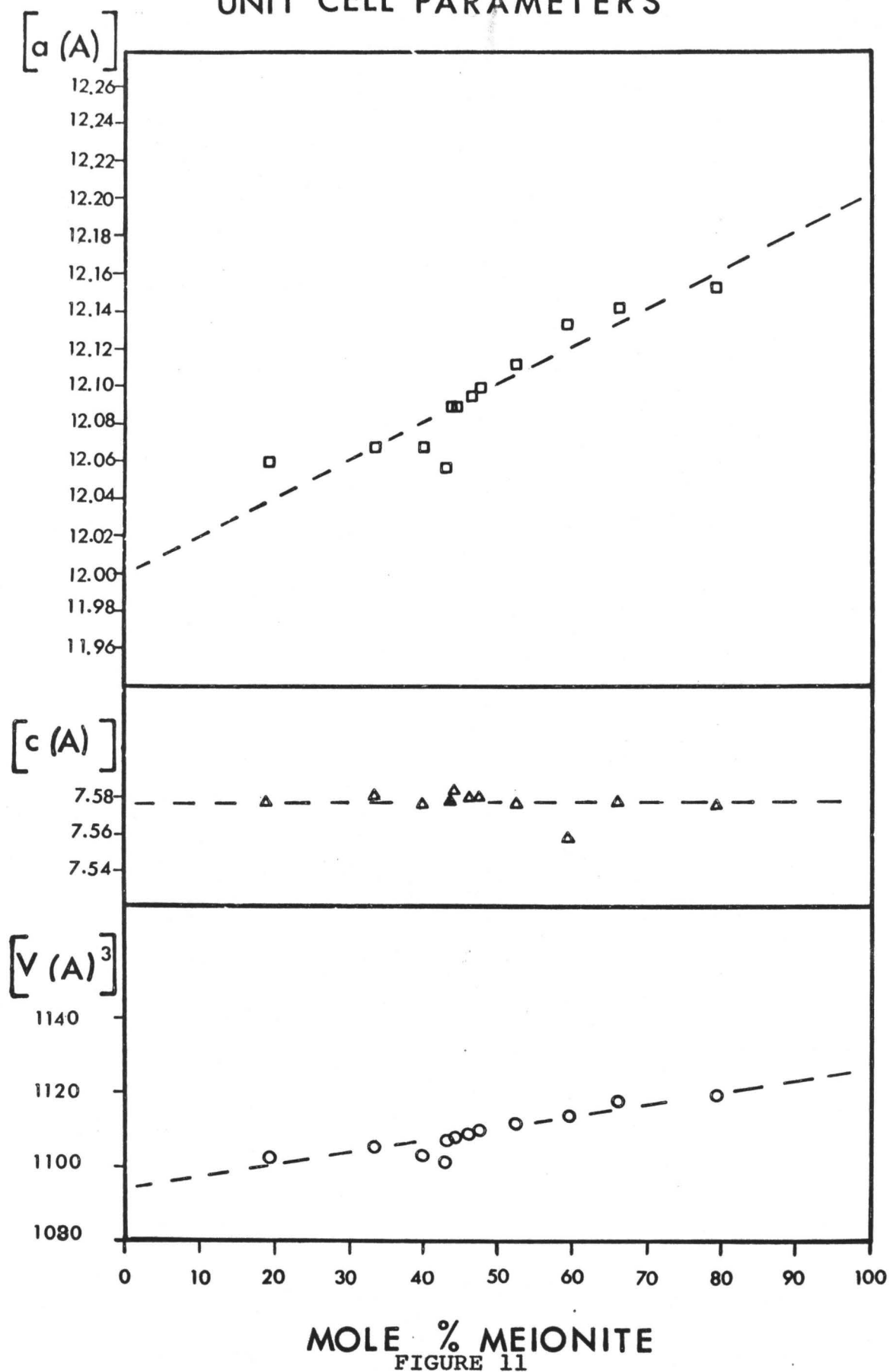


FIGURE 11

PROBE STUDIES

The Electron Probe Microanalyzer.

General: The first electron probe x-ray microanalyzer was developed in France by R. Castaing (1951). Castaing and Guinier were the first to demonstrate that a small polished specimen could be analyzed locally by means of x-ray emission. They also developed expressions which relate x-ray intensities to chemical composition. The probe itself consists of an electron optical system coordinated with both reflected and transmitted light microscopes. The surface analyzed may thus be observed during analysis of the specimen, which is mounted in a specimen stage at the base of the electron optic column. Upon focussing an electron beam upon the surface of the specimen (preferably polished) characteristic x-rays corresponding to elements present are given off from a minute bulb-shaped volume in the specimen. The x-rays transmitted from the specimen are sensed by detectors, either flow or proportional counters. The output of the spectrometer when compared to x-ray emission intensities from suitable standards is a measure of the

relative or absolute concentration of an element within a specimen.

Specifics: The electron probe microanalyzer is composed of the following systems:

1. Electron optics.
2. Light optics.
3. X-ray optics.
4. Specimen and vacuum system.
5. Analyzing electronics.

Electron Optics: The electron optics consist of a tungsten cathode mounted above a Wehnelt cylinder which is at a more negative potential than the cathode filaments allowing control of the beam current from the filament. This allows production of a stable emission current through the use of a feedback system. Figure 12. illustrates the geometry of the system. Note the magnetic lenses which regulate the size and geometry of the electron beam. The condenser lens has a variable focal length of two to one hundred millimeters. The objective lens has a coaxial fitting for the optical reflection type microscope. The focal length of this lens is nine

FIGURE 12

A schematic diagram of the electron
probe x-ray microanalyzer.

MICROANALYZER SCHEMATIC DIAGRAM

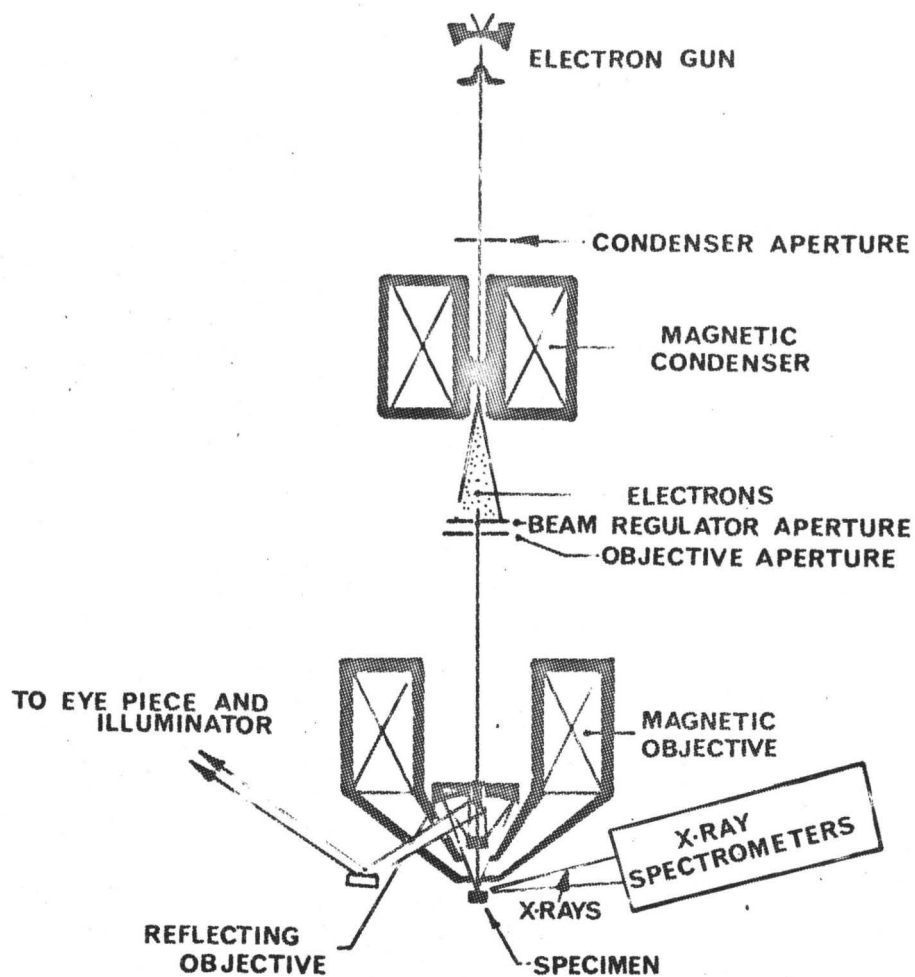


FIGURE 12

millimeters. It might be noted that the first lens or condenser lens determines the minimum probe size, whereas the second reducing lens, the objective lens focuses the spot on the specimen. The electron optics as well as the above features, includes an astigmatism corrector and an arrangement for beam scanning. Beam scanning is achieved by applying signal voltages to four plates built into the objective system.

Light Optics: As mentioned previously the reflected light optics uses a coaxial mirror objective. This enables the operator to observe the specimen during analysis. The actual resolution claimed by the optical system is 0.5 microns. Binocular eyepieces enable a magnification of 400 diameters. Transmitted light optics are also included. Circular polarized light may be used at will. The transmitted light optics while not as excellent as that found in a petrological microscope are sufficient for identification purposes of scapolite and plagioclase.

X-ray Optics: The MS-64 Acton probe has four spectrometers; two of these spectrometers are flow proportional counters and two are sealed proportional counters. The window between the evacuated chamber

housing the flow counters and the column was of stretched mylar film. The window for the sealed counters was beryllium.

We were not able to maintain a collodion window for the analysis of calcium however a stretched mylar window was found to be adequate. Analysis of calcium was undertaken using a mica crystal (mica monochrometers have a maximum error of 0.002 angstroms). A fully focussing spectograph is required in measuring x-ray intensities because the point of impact is five orders of magnitude less than that of a conventional x-ray tube. All spectrometers in the instrument used accept x-rays from the specimen at a take-off angle of 18° .

Specimen Chamber and Vacuum System: The specimen chamber is located at the base of the probe column. The specimen stage motion allows a movement of one inch in the x direction, two inches in the y and focussing adjustment of ± 0.75 millimeters. Using the calibrated controls the x and y coordinates may be duplicated in any one specimen to \pm one micron. A stepping drive is also available allowing movement of the specimen automatically beneath the electron beam. The vacuum system in the MS-64 consists of two independent vacuum systems. The pumping

rate for the electron optic column and spectrometer housings is 5 cubic feet per minute, mechanical pump and 750 liters per second diffusion pump. The system is interlocking therefore operator errors could not harm the equipment. Pump down time is approximately 30 minutes. However, when exchanging specimens the spectrometer housings can be isolated from the probe. Thus on changing specimens it is only necessary to pump down the column.

Analyzing Electronics: The electronics equipment is produced by Phillips and consists of four preamplifiers and two analyzing channels. This includes a linear amplifier, a pulse height analyzer, a linear ratemeter, a high speed scaler, a two-pen strip chart recorder, a dual high voltage power supply and one high speed electronic timer.

Analytical Procedure.

In this study CaK_{α_1} intensities were used to determine the mole percentages of Ca in scapolite and plagioclase. All analyses utilized an accelerating voltage of 26 KV and a beam current of 100 nanoamps. (1 n amp = 1/1000 u amp) and a spot size ranging in magnitude from 1 to 5 microns depending upon conditions of analysis.

When analyzing individual grains within a thin section or mounted in a polished section 10 ten second counts were made on each grain at different points throughout the grain. Scalers were used for such an analysis. Since surface conditions such as topography or contamination were found to affect the count rate a stationary spot was used. Drift corrections were applied to the readings. The drift was determined by repeatedly analyzing one mineral standard in a specific area during successive intervals throughout the analysis. Since abundant standards were available, there was no need to apply absorption or fluorescence corrections to the intensities. Generally, calibration curves were plotted using I/I_0 as the ordinate function and using mole percentage meionite for the abscissa. I_0 is the intensity of $\text{CaK}\alpha_1$ radiation from a suitable end member. Using this technique it was possible to compare calibration curves obtained under different conditions. Error was noted to be ± 2.5 mole per cent meionite. It must be noted that a large factor affecting precision in the Acton probe is the inability to duplicate exactly the focus for each separate analysis. This problem was only realized after discussing this factor with operators

of different electron probes. All samples analyzed were coated with a thin coat of carbon using an evaporator. When coating the sample it was noted that the colours of the spectrum could be observed, the colours seen depending upon the thickness of the carbon coat. Evaporation was thus halted when a straw yellow colour was observed. To obtain uniformity both standards and samples were coated simultaneously. This was done to eliminate or reduce any errors due to thickness variations of the conducting carbon coat between the standard and the samples.

Mounting of Standards.

Standards used were mounted in brass plates having a width of one inch and a maximum length of two inches. (Plate 1). Holes were drilled in the brass plates. These holes were then half-filled with epoxy. When the epoxy hardened the standard was then placed upon this semi-translucent base. The diameter of holes drilled was varied depending upon the sample size and the number of standard grains to be mounted. Epoxy was poured around the standard grain and allowed to harden. A small volume of the grain was allowed to project above the surface of the sample holder. This excess volume was partially removed by grinding on a medium grade diamond impregnated

PLATE 1

This plate illustrates:

- a) A typical standard holder containing six polished standards
- b) A screw type standard holder which may be used to hold twenty four standards. Note the depressed region around the cups. This type of holder proved unsatisfactory due to the rotation of the cups when polishing was undertaken.
- c) A standard holder similar to that in a). This holder was inserted in the slide clips in place of the slide.
- d) The sample and standard holder used in the Acton probe. Note that a standard of type a) and a polished thin section are in place.

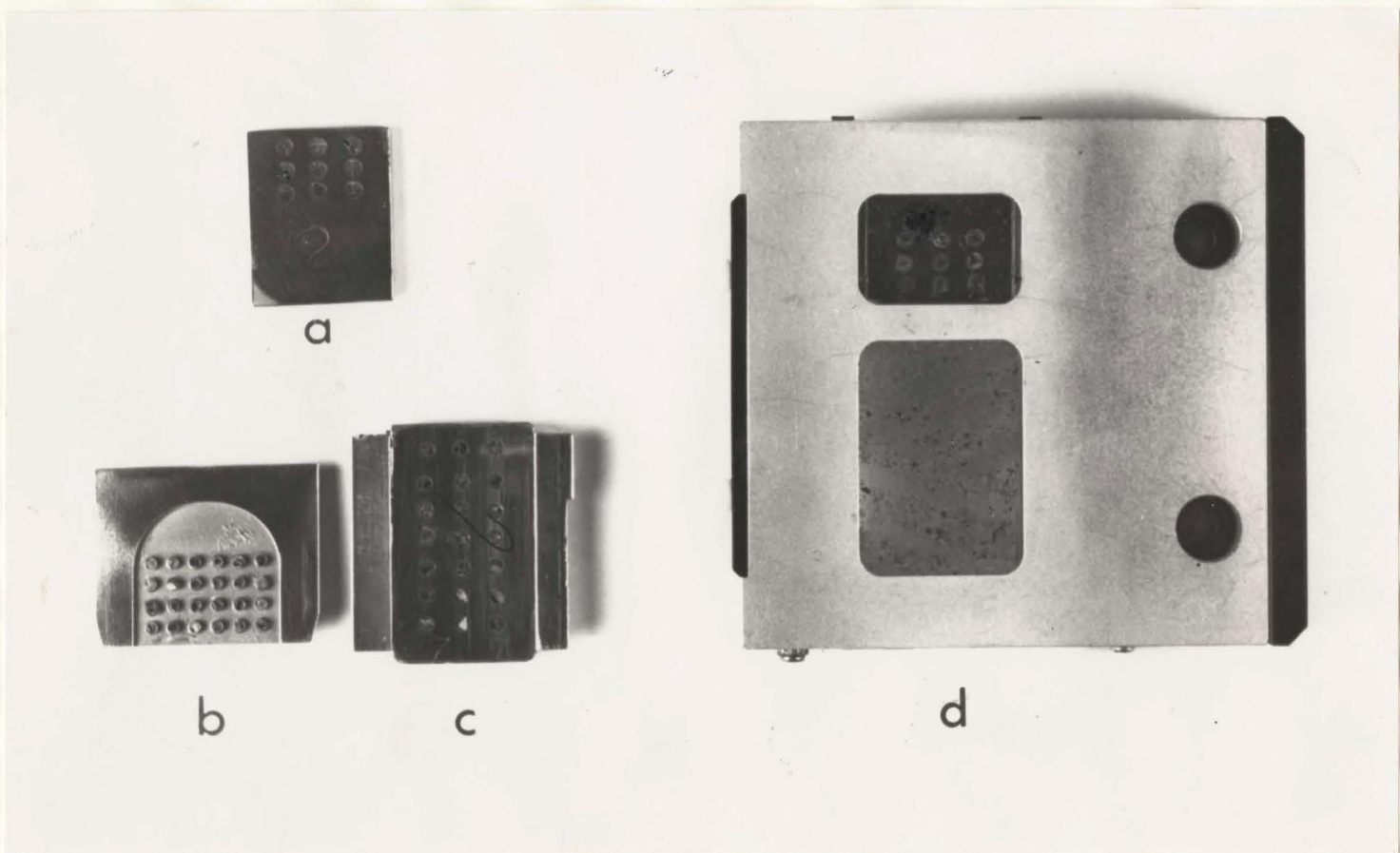


PLATE 1

wheel. The samples were then polished flush with the brass holder using 9 micron silica carbide placed on a glass plate. The standard was then polished to a final $\frac{1}{4}$ micron polish using nylon cloths on a brass wheel. Diamond paste was placed on the nylon lap which was then dampened with polishing oil. The grades of diamond used were 5, 1 and $\frac{1}{4}$ micron. Between each stage the sample was cleaned by means of an ultrasonic probe. The specimen or holder was immersed in soapy water; the probe was then inserted and operated at a high frequency. This operation completely removed any oil or contamination on the sample.

Preparation of Polished Thin Sections.

Those rock samples which were to be studied were cored to obtain fresh specimens by means of a one inch diameter diamond bit which was attached to a drill press. The cores were cut and sectioned to a suitable size for polishing. Some of the cores were cut lengthwise, others crosswise depending upon orientation of the sample. The surface to be polished was subjected to the following procedures:

1. Coarse, medium and fine grinding on diamond impregnated aluminum backed wheels.
2. Further grinding using 4 micron SiC on a nylon lap.

3. Polishing on a nylon lap using 9 micron diamond paste.
4. Polishing on a nylon lap using 1 micron diamond paste.
5. Polishing on a nylon lap using $\frac{1}{4}$ micron diamond paste.

Each polishing and grinding stage required a minimum of five minutes. Heavy pressure was applied at all stages. Between each stage the specimen was cleaned in a detergent solution using the ultrasonic probe. The polished surface obtained was glued to a glass slide using 70° Lakeside cement. The mounted specimen was then ground to .03 millimeters thickness. Vaseline was then smeared around the thin section. A clear epoxy which had been diluted with methyl hydrate was then smeared on the ground surface of the rock slice. The specimen was then placed against a clean microscope slide. The epoxy was allowed to harden overnight. The slide was next heated to above 70°C. This melted the Lakeside cement and hence exposed the polished surface. This surface was cleaned by washing with methyl hydrate, acetone and petroleum ether. After the vigorous application of each solvent the polished surface was subjected to an air blast to promote evaporation and to remove grit deposited on the polished surface.

Calibration Curves and Determination of Homogeneity.

Scapolite Standards: All of the standards were analyzed for Ca using two spectrometers, one containing a mica crystal and the other a quartz crystal. Figures 13 and 14 show the results of counts per second CaK_{α_1} versus mole per cent meionite using the above crystals.

It is unusual that the intensities of the CaK_{α_1} radiation using the mica crystal did not extrapolate to zero for this particular set of analyses. This bears further investigation.

Since as Figures 13 and 14 illustrate, effects of fluorescence and absorption are negligible a linear relation was assumed to exist between CaK_{α_1} intensity and mole per cent meionite. Sodium was not analyzed since volatilization occurred in sodium rich samples.

Standards ON 8, Q 87, and ON 47 were chosen as working standards to establish a working curve plotting I/I_0 versus mole per cent meionite, where $I = \text{Ca K}_{\alpha_1}$ intensity and $I_0 = \text{CaK}_{\alpha_1}$ intensity from ON 47. Ten ten second counts were made at various random points throughout each standard and counts were averaged for each standard.

FIGURE 13

Calibration Curve Utilizing Mica Crystal.

CaK_{α_1} Intensity vs Mole % Meionite.

Note that this curve has not been corrected for background. Background using the mica crystal appears to be extremely great. The cause of this requires investigation.

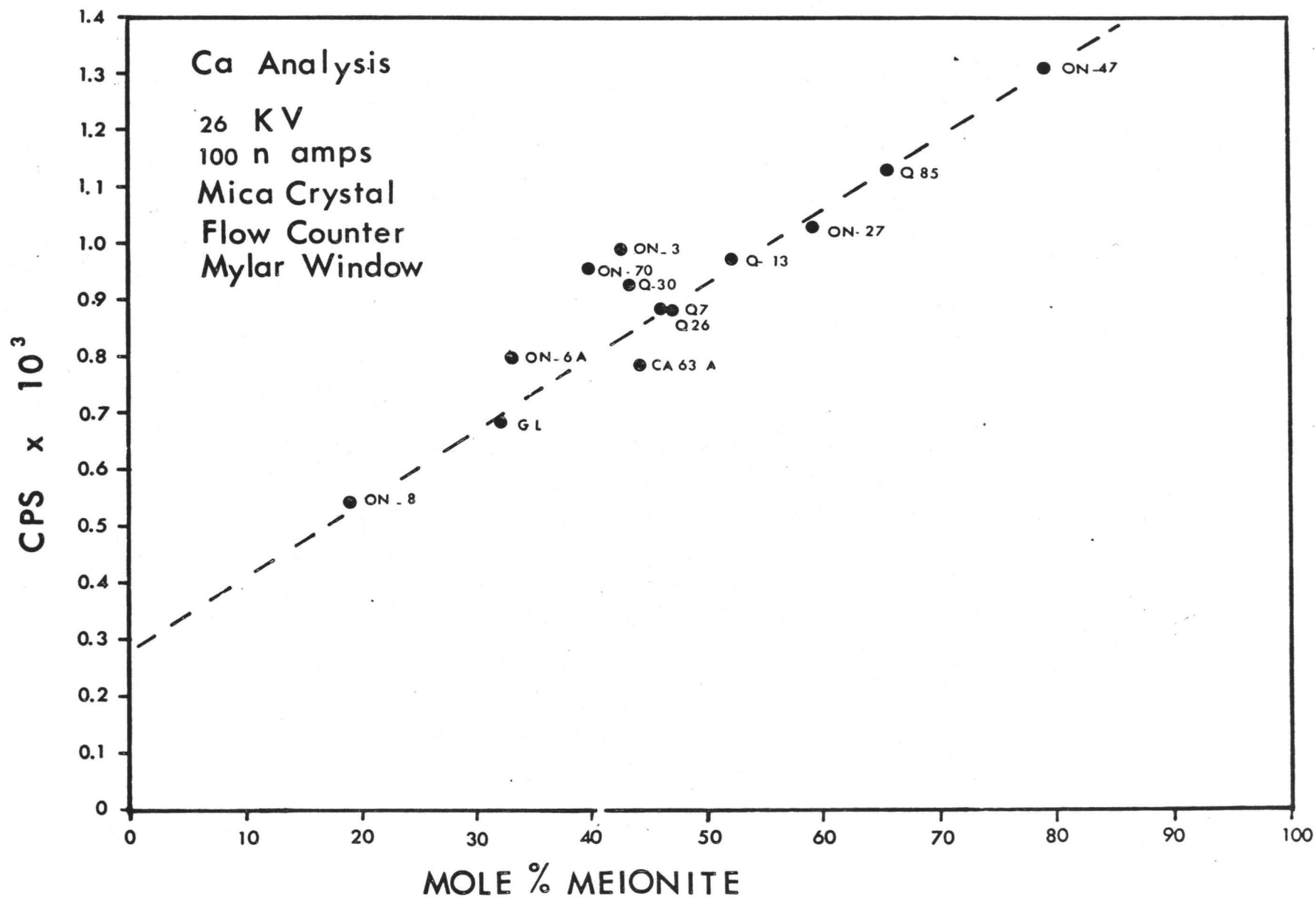


FIGURE 13

FIGURE 14

Calibration Curve Utilizing Quartz $10\bar{1}1$

CaK_{α_1} Intensity vs Mole % Meionite.

Note that this curve extrapolates to zero. No correction was made for background.

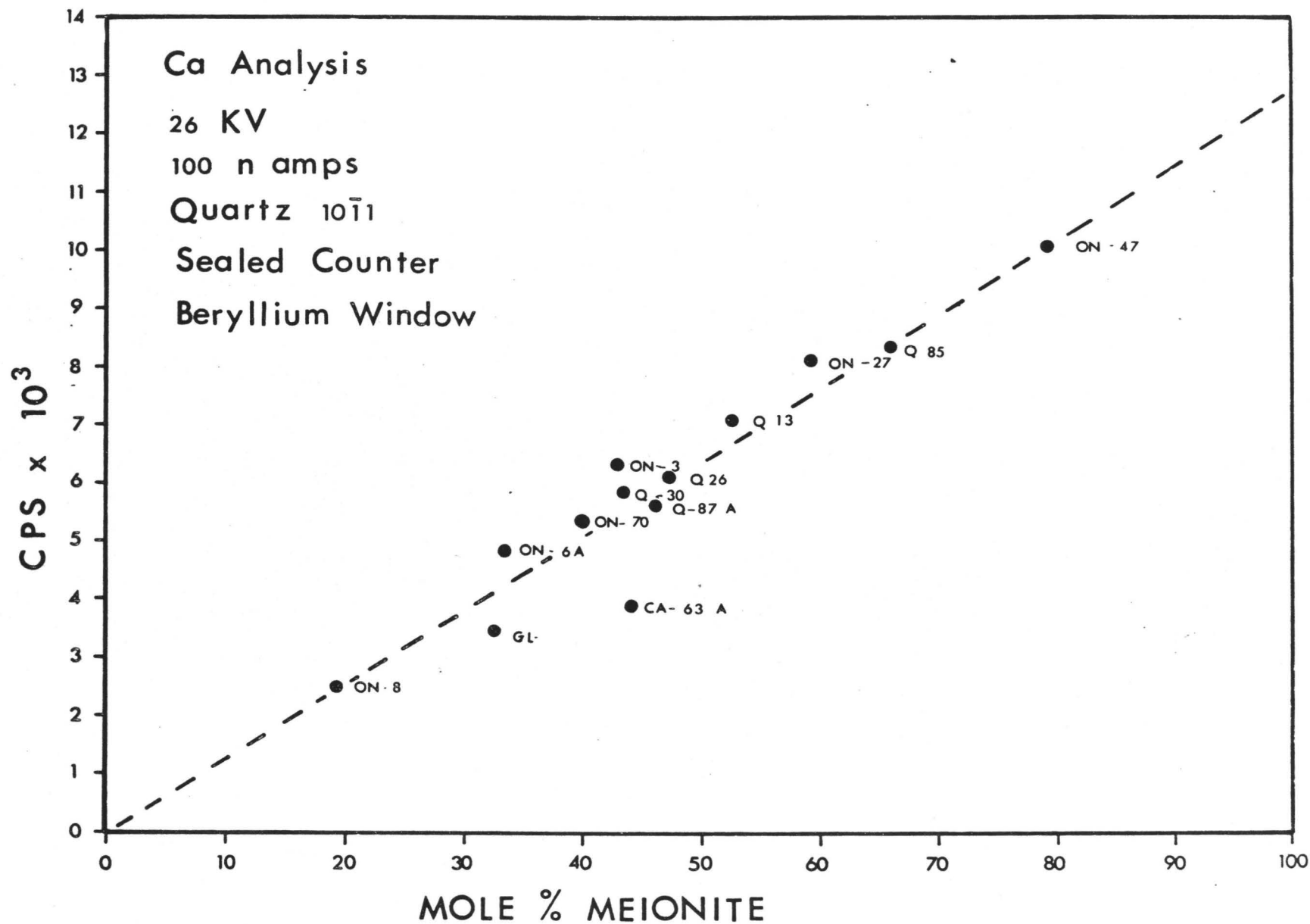


FIGURE 14

In order to test the homogeneity of the standards scans were made across the surface of each standard as illustrated in Figures 15 to 24.

It may be noted that the intensity of radiation is proportional to the amount of calcium in the samples. Obvious irregularities are explained by inclusions or foreign substances on the surface of the standard or necessary adjustments in focus. The mica crystal was used for routine analysis.

FIGURES 15-24

Scale 1 inch = 93 microns.

Scans across scapolite standards
indicating lack of zoning.

Analysis for $\text{CaK}_{\alpha 1}$

Mica Crystal

26 KV

100 nanno amps.

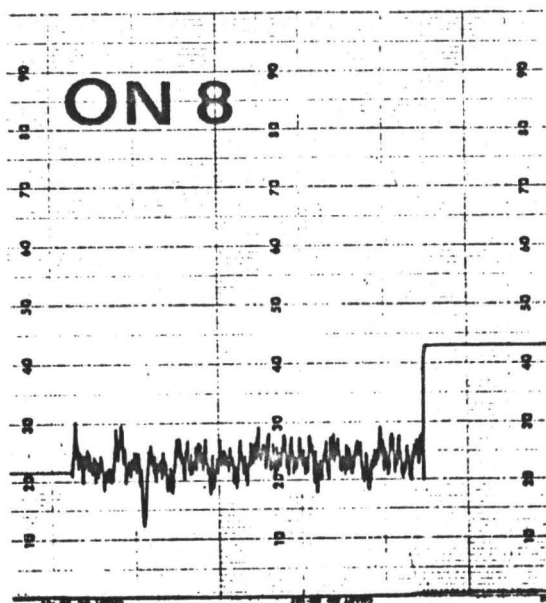


FIGURE 15
 Mole % Me = 19.4
 Wt. % CaO = 4.81

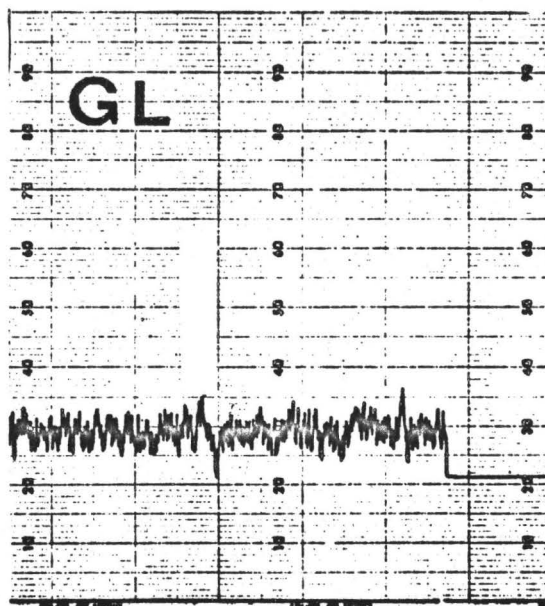


FIGURE 16
 Mole % Me = 32.5
 Wt. % CaO = 7.2

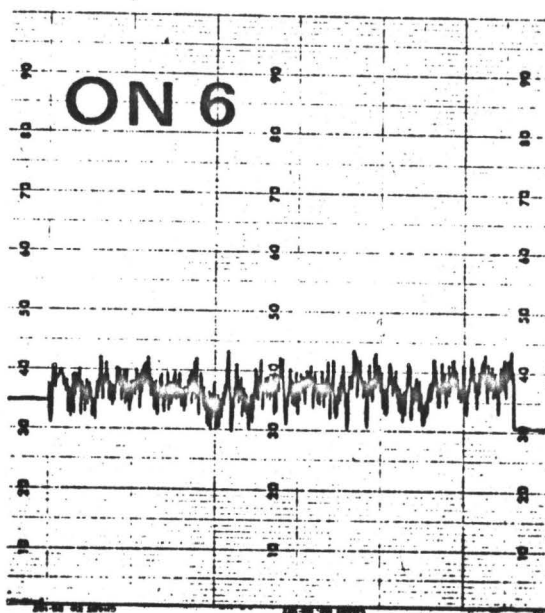


FIGURE 17
 Mole % Me = 33.5
 Wt. % CaO = 8.29

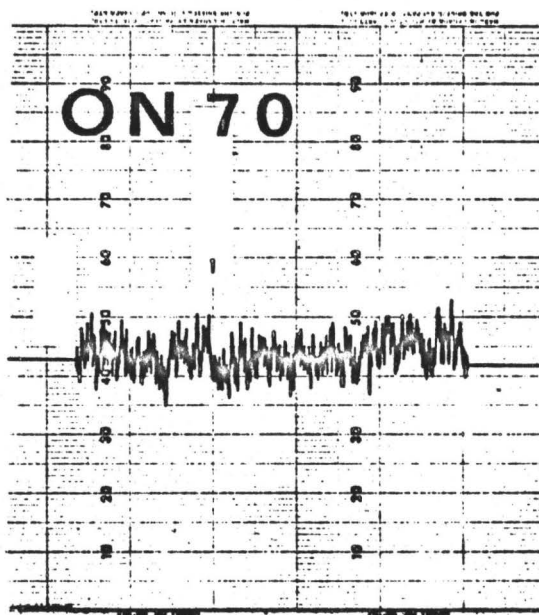


FIGURE 18
 1. Focus adjusted.
 Mole % Me = 40.18
 Wt. % CaO = 9.88

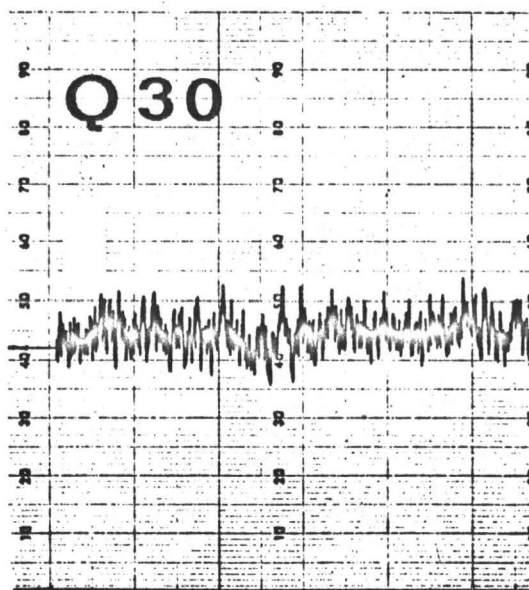


FIGURE 19

Mole % Me = 43.69

Wt. % CaO = 10.45

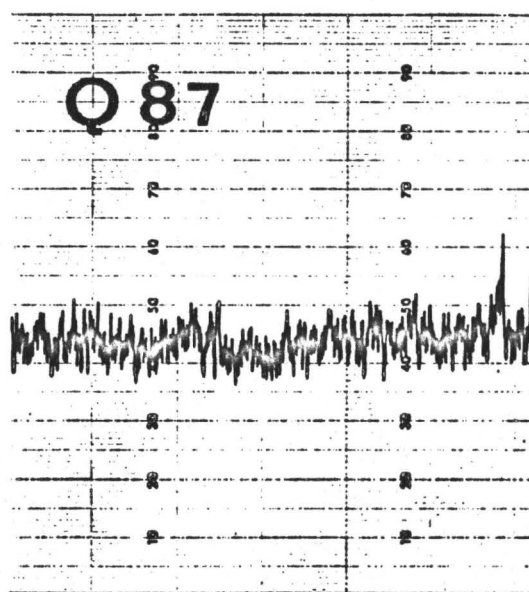


FIGURE 20

Mole % Me = 46.2

Wt. % CaO = 11.13

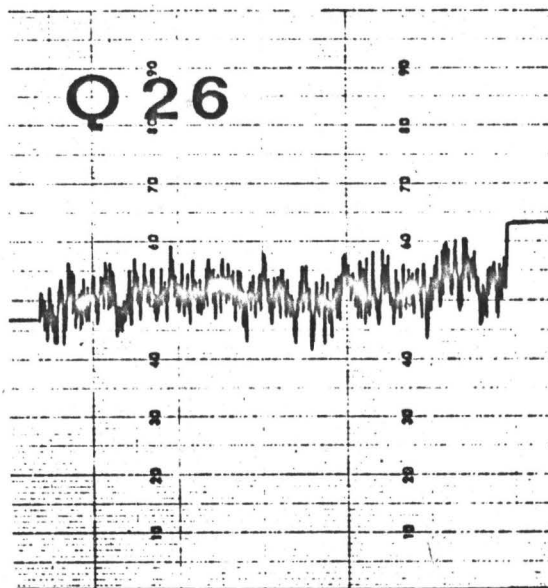


FIGURE 21
Mole % Me = 47.46
Wt. % CaO = 11.30

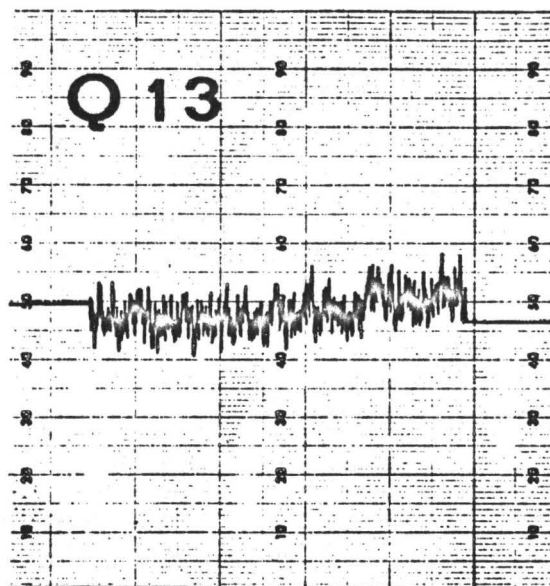


FIGURE 22
Mole % Me = 52.58
Wt. % CaO = 12.56

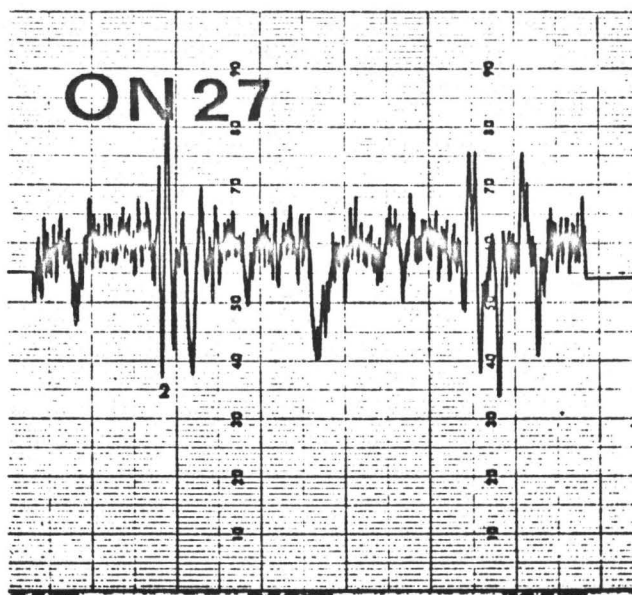


FIGURE 23
 2. Oil on surface of section.
 Mole % Me = 59.30
 Wt. % CaO = 14.11

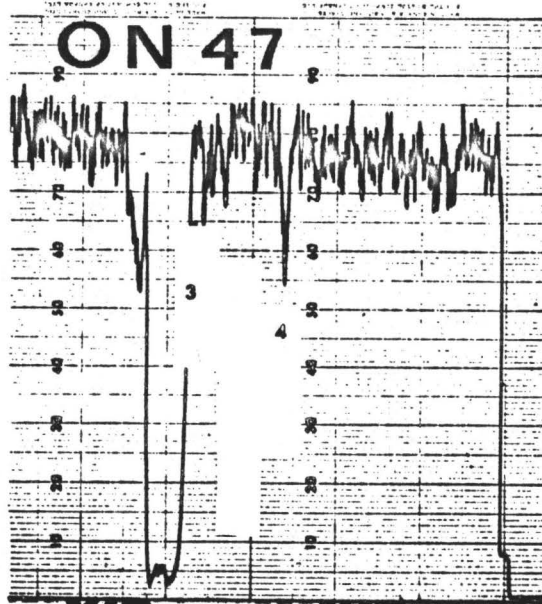


FIGURE 24
 3. Inclusion.
 4. Crevice
 Mole % Me = 79.34
 Wt. % CaO = 18.65

Plagioclase Standards: The plagioclase standards as previously mentioned were supplied by D. Lindsley, Geophysical Laboratory Washington. These samples cover 10 mole per cent intervals from 0 to 100 mole per cent anorthite. Since volatilization of Na occurred in sodium rich samples, analysis of calcium was used as the sole means of determining mole per cent anorthite. Calibration curves for these glasses have not been included as they are essentially linear and such a presentation would be duplication of those results obtained by J.V. Smith (1966). An_0 , An_{100} and two other arbitrarily selected plagioclase samples were used as working standards. As in the case of scapolite analysis, 10 ten second counts were made on each grain and the results of each determination averaged. A working curve was established with I_0 determined from An_{100} . I/I_0 was plotted versus mole per cent anorthite (as before $I = CaK_{\alpha 1}$ intensity). Drift was also recorded by means of analysis of an arbitrary plagioclase reference standard. Error was estimated as ± 2 mole per cent anorthite.

Sample Sources.

D.M. Shaw contributed the majority of samples

from which polished thin sections were made. Other contributors were I.M. Mason, E.L. Speelman, D.Jennings, (all of McMaster University) R.Bradshaw (University of Bristol,England) and A.W. Kleeman, (University of Adelaide, Australia). Metamorphic grade in these samples varied from that of the amphibolite to that of the granulite facies.

Localities, where known, and sample descriptions have been listed in Table 9.

TABLE 9
Localities of Scapolite Bearing Rocks
(Samples Containing Both Plagioclase and Scapolite)

Sample	Rock Type	Locality
Donor <u>D.M.S.</u>		
CA 30	Scapolite-Pyroxene Gneiss	Grand Calumet Twp., P.Q.
CA 40	Garnet-Scapolite-Quartz Gneiss	"
CA 63B	Skarn Rock: Scapolite, Diopside, Plagioclase.	"
CA 75	Skarn Rock: Hornblende, Plagioclase, Sphene.	"
CA 76	Hedenbergite-Hornblende Sphene Gneiss	"
68-81-8	Scapolite-Hornblende-Quartz Epidote Gneiss	Chandos Twp. Ontario.
69-28-6A	Scapolite Marble	"
69-35-4	Augite-Quartz-Biotite Scapolite-Plagioclase Schist	"
69-35-5	Quartz-Plagioclase-Scapolite- Pyroxene Granulite	"
70-146-5	Hornblende-Biotite Schist	"
70-148-3	Hornblende-Plagioclase-Scapolite Gneiss	"
72-198-2	Quartz-Scapolite-Hornblende- Pyroxene-Microcline-Plagioclase Granulite	"
72-202-5	Augite-Scapolite-Garnet Skarn Rock	"
73-110-2	Biotite-Hornblende-Pyroxene Scapolite-Plagioclase Granulite	"

TABLE 9

Sample	Rock Type	Locality
Donor		
<u>I. Mason</u>		
3	Anorthosite: Plagioclase Diopside	Anorthosite in McKenzie,
8	" Hornblende	Hagerman, Buree
10	" Scapolite	and Ferguson Twps. Ontario
14	"	"
16	"	"
27	"	"
111	Scapolite-Garnet-Plagioclase Gneiss	"
205	Anorthosite	"
209	"	"
226	"	"
353	"	"
355	"	"
356	"	"
357	"	"
381	"	"
Donor		
<u>E. Speelman</u>		
	Anorthosite: Plagioclase Hornblende	
S-44	" Biotite	Minden Twp., Ontario.
S-48	" Scapolite (Diopside)	"
S-49	"	"
S-51	"	"
S-53	"	"

TABLE 9 CONT'D

Sample	Rock Type	Locality
S-54	Anorthosite	Minden Twp. Ontario
S-105	Microcline-Biotite-Quartz Gneiss	Chandos Twp. Ontario.
S-162	Plagioclase-Quartz-Biotite Hornblende Gneiss	Wollaston Twp. Ontario.
S-164	Diopside-Plagioclase-Scapolite Gneiss	"
S-165	Plagioclase-Quartz-Biotite Hornblende Gneiss	"
Donor <u>R. Bradshaw</u>		
193	Scapolite-Biotite-Hornblende Gneiss	Near the village Sørfinnset, County Gildeskool Norway
194	Scapolite-Biotite-Hornblende- Plagioclase Gneiss	"
230	Quartz-Biotite-Plagioclase- Scapolite-Hornblende Gneiss	"
256	Quartz-Biotite-Hornblende Garnet Gneiss	"

Samples Containing Scapolite

Donor D.M. Shaw		
CA 1	Pyroxenite	Grand Calumet Twp. P.Q.
CA 19	Skarn	"

TABLE 9 CONT'D

Sample	Rock Type	Locality
CA 56	Scapolite-Diopside Gneiss	"
CA 81B	Pyroxene-Scapolite Gneiss	"
CA 105 B	Scapolite Gneiss	"
D 1	Pyroxene-Scapolite-Calcite Granulite	unknown
ON 19	Pyroxene-Garnet Skarn	Monmouth Twp. Ontario
ON 22	Pyroxene Marble	Glamorgan Twp. Ontario
ON 34	Scapolite-Pyroxene-Calcite Gneiss	"
Q 7	Pargasite-Diopside Scapolite Skarn	Huddersfield Twp. P.Q.
Q 24 C	Scapolite-Pyroxene Granite	Clapham Twp. P.Q.
Q 27	Pegmatitic Skarn	Huddersfield Twp. P.Q.
Q 31 B	Scapolite-Epidote Gneiss	Clarendon Twp. P.Q.
P-1	Scapolite-Pyroxene Gneiss	Unknown
68-81-8	Scapolite-Quartz-Epidote Gneiss	Chandos Twp. Ontario.
69-53-6	Pyroxene-Scapolite Gneiss	"
70-143-8	Pyroxene-Scapolite-Quartz Gneiss	"
70-146-4	Scapolite-Pyroxene Gneiss	"

TABLE 9 CONT'D

Sample	Rock Type	Locality
70-147-1A	Calcite-Scapolite-Diopside Gneiss.	"
71-50-7	Scapolite-Augite-Epidote-Quartz Granulite	"
630628-1	Hornblende-Microcline-Biotite-Quartz Schist	"
Donor <u>D.Jennings</u>		
3An-34	Scapolite Amphibolite	Anstruther Twp. Ontario.
Donor <u>A.Kleeman</u>		
PV 17	Scapolite-Hornblende-Diopside Gneiss	Flinders Range South Australia
157-48-A	Scapolite Gneiss	"
KS	Scapolite Gneiss	"
9250	Pyroxene-Scapolite Gneiss	"
Donor <u>E.Speelman</u>		
S 16-3	Scapolite-Diopside Gneiss	Unknown

Plagioclase Scapolite Analysis.

The results of the analyses of plagioclase-scapolite rocks are listed in Table 10. In presenting data a mean of ten or fewer analyses was used to represent the composition of the feldspar or scapolite in the rock. Where possible plagioclase scapolite grains in contact were analyzed. No plagioclase and scapolite grains were compared if these minerals appeared in separate gneissic bands. The results of probe analyses of scapolite in rocks containing no plagioclase has been presented in Table 11. The latter analyses were made primarily for the purpose of determining the compositional range of scapolite in these samples.

Discussion of Plagioclase-Scapolite Analysis:

Plotting the mole per cent melonite versus mole per cent anorthite Figure 25 is obtained. Points falling above a 45° line indicate that scapolite is more calcic than coexisting plagioclase. The various sources have been indicated by the appropriate symbols. From this graph the following conclusions may be drawn:

1. Scapolite is generally more calcium rich than coexisting plagioclase.
2. There is a general tendency for Ca-rich scapolite to coexist with Ca-rich plagioclase.

TABLE 10
Coexisting Scapolite and Plagioclase
Analysis by Microprobe (D.R.H.)

Sample	Mean	# of Scap-Plag Pairs	Standard Deviation	K'
<u>Donor D.M. Shaw</u>				
CA 30 (S) *	62.3	3	2.7	1.30
" (P) *	56.1		2.8	
CA 40 (S)	67.10	4	1.36	4.81
" (P)	29.78		2.43	
CA 63B (S)	34.40	2	3.11	2.29
" (P)	18.65		3.89	
CA 75 (S)	54.9	10	6.6	1.32
" (P)	48.0		6.2	
CA 76 (S)	59.2	7	5.3	2.30
" (P)	38.7		1.8	
68-81-8 (S)	68.3	10	11.3	3.10
" (P)	41.0		4.3	
69-28-6A (S)	57.9	10	1.9	2.62
" (P)	34.4		1.3	
69-35-4 (S)	64.9	6	3.6	2.08
" (P)	47.1		3.4	
69-35-5 (S)	63.3	7	8.9	0.93
" (P)	64.9		3.8	
70-146-5 (S)	41.7	3	1.7	1.62
" (P)	30.7		0.3	
70-148-3 (S)	59.6	4	1.0	1.80
" (P)	45.0		1.6	
72-198-2 (S)	63.1	9	4.9	3.37
" (P)	33.6		1.9	
72-202-5 (S)	73.0	4	3.9	4.90
" (P)	35.5		1.1	

TABLE 10 CONT'D

Sample	Mean	# of Scap-Plag Pairs	Standard Deviation	K'
73-110-2 (S)	83.5	10	2.9	11.28
" (P)	31.0		4.3	
<u>Donor I.M.Mason</u>				
3 (S)	82.7	4	4.4	2.46
" (P)	66.1		1.9	
8 (S)	83.2	4	4.3	3.44
" (P)	59.1		4.9	
10 (S)	73.5	4	9.2	1.82
" (P)	60.4		1.3	
14 (S)	70.7	10	3.8	1.28
" (P)	65.3		2.04	
16 (S)	73.4	9	5.3	1.76
" (P)	61.1		2.8	
27 (S)	79.69	9	4.0	2.54
" (P)	60.8		4.9	
111 (S)	76.2	9	4.2	3.48
" (P)	47.9		6.4	
205 (S)	78.5	10	5.1	3.47
" (P)	51.2		4.2	
209 (S)	72.1	10	14.0	1.42
" (P)	64.5		3.9	
226 (S)	77.3	10	4.9	3.44
" (P)	49.7		2.7	
353 (S)	75.8	10	7.7	2.54
" (P)	55.2		3.0	
355 (S)	75.2	10	4.6	1.49
" (P)	67.0		3.8	
356 (S)	78.3	10	8.2	2.96
" (P)	54.9		3.4	

TABLE 10 CONT'D

Sample	Mean	# of Scap-Plag Pairs	Standard Deviation	K'
357 (S)	80.6	10	3.3	0.83
" (P)	83.4		4.5	
381 (S)	75.2	10	3.8	2.91
" (P)	51.0		6.6	
<u>Donor R. Bradshaw</u>				
193 (S)	76.0	10	3.2	1.65
" (P)	65.7		2.2	
194 (S)	80.0	10	7.1	2.73
" (P)	59.4		8.5	
230 (S)	78.8	6	4.7	5.75
" (P)	39.3		0.9	
256 (S)	65.1	2	1.6	0.95
" (P)	66.2		2.6	
<u>Donor E.L. Speelman</u>				
S44 (S)	69.8	10	1.8	1.98
" (P)	53.9		2.9	
S48 (S)	75.6	10	4.01	1.64
" (P)	65.4		3.9	
S49 (S)	71.8	10	1.4	2.28
" (P)	52.7		4.5	
S51 (S)	72.9	9	3.8	0.39
" (P)	87.3		3.2	
S53 (S)	65.3	10	2.3	1.52
" (P)	55.4		2.8	
S54 (S)	70.2	10	4.3	2.86
" (P)	45.2		2.7	
S105 (S)	61.6	5	3.2	1.33
" (P)	54.7		2.9	

TABLE 10 CONT'D

Sample	Mean	# of Scap-Plag Pairs	Standard Deviation	K'
S 162 (S)	54.8	10	1.8	1.66
" (P)	42.3		2.1	
S 164 (S)	72.0	10	3.8	2.69
" (P)	48.9		2.2	
S 165 (S)	73.6	10	6.7	2.60
" (P)	51.8		3.7	

* (S) indicates mole per cent meionite
 (P) indicates mole per cent anorthite

TABLE 11
Scapolite Analyses by Microprobe (D.R.H.)

Sample	# of analyses	Mean Mole % Me	Standard Deviation
<u>Donor D.M.Shaw</u>			
CA 1	4	17.2	2.5
CA 19	5	33.9	4.3
CA 56	5	54.4	1.8
CA 81B	5	32.4	1.4
CA 105B	5	58.3	2.2
D 1	4	52.3	2.2
ON 19	5	63.5	8.9
ON 22	5	54.0	2.2
ON 34	4	56.5	0.9
Q 7	5	67.8	2.2
Q 24C	5	47.4	0.7
Q 27	5	42.0	1.3
Q 31B	5	34.7	1.7
P 1	5	40.1	5.1
68-81-8	5	81.5	2.9
69-53-6	5	54.9	0.89
70-143-8	5	73.9	2.0
70-146-4	5	53.2	8.0
70-147-1A	5	64.4	0.7
71-50-7	5	67.3	2.4
630628	5	59.1	2.2
<u>Donor D.Jennings</u>			
3An-34	5	57.0	2.1
<u>Donor A.W.Kleeman</u>			
PV 17	5	55.7	1.6
157-48-A	5	61.0	2.3
KS	5	46.0	1.7
9250	5	65.3	1.7
<u>Donor E.L.Speelman</u>			
S 16-3	5	59.0	1.0

FIGURE 25

Mole % Me vs Mole % An

Note: All scapolite samples above the indicated 45° line are richer in Ca than the coexisting plagioclase.

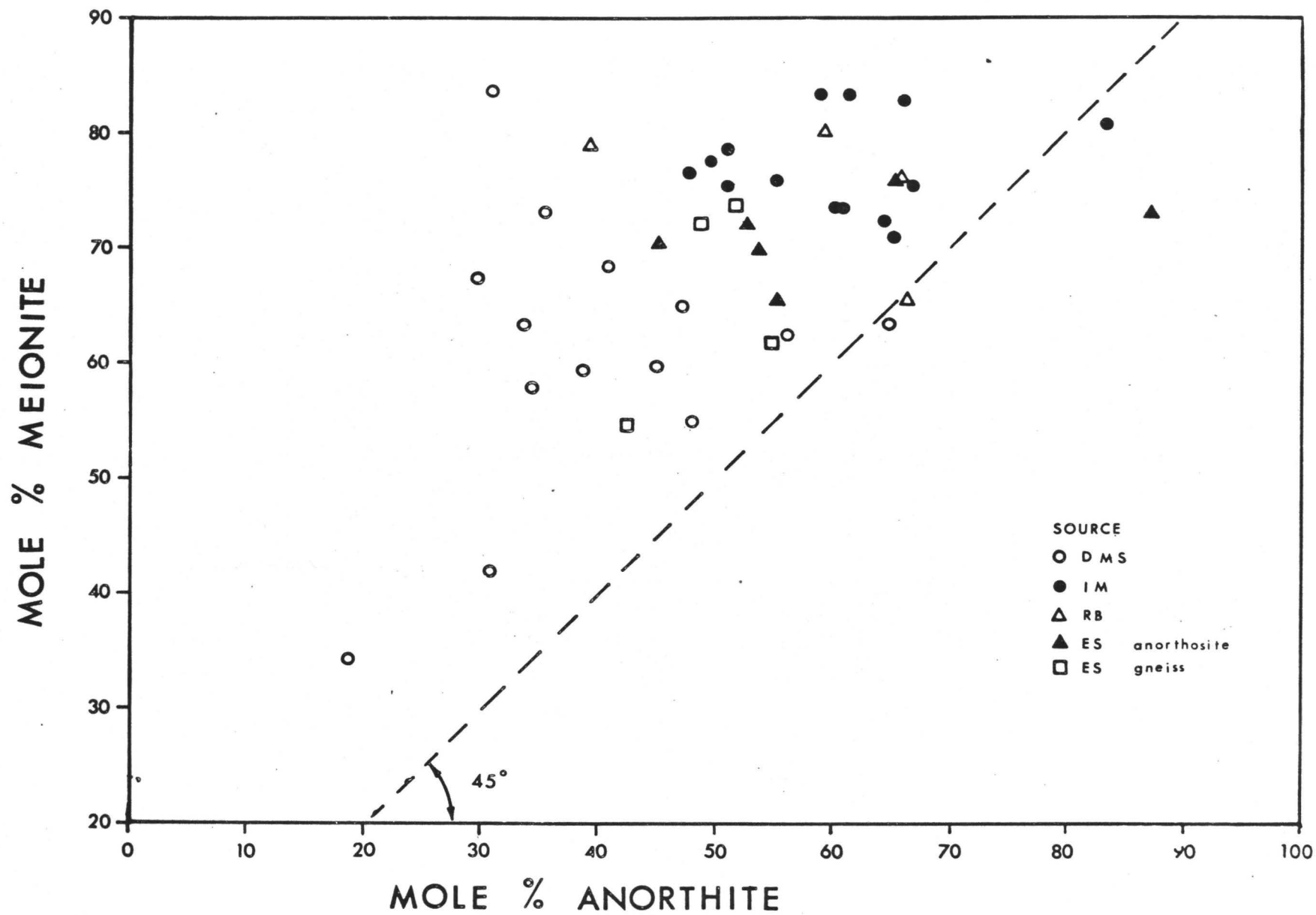


FIGURE 25

The Equilibrium Coefficient: In an exchange reaction of the type



where A and B represent components and ()Z, ()W represent phases, the following equation applies:

$$\Delta G = \Delta G^{\circ} + RT \ln \frac{Q_B^Z \cdot Q_A^W}{Q_A^Z \cdot Q_B^W}$$

where ΔG = the free energy change of reaction and

ΔG° = the standard state Gibbs free energy change.

$$Q_B^Z = \text{activity of B in phase Z} = \gamma_B^Z \chi_B^Z$$

γ = activity coefficient

χ_B^Z = mole fraction of B in Z

Note: $\chi_B^Z + \chi_A^Z = 1$

also $\chi_B^W + \chi_A^W = 1$

By definition $\Delta G = 0$ at equilibrium, also for an ideal solution $\gamma = 1$ for all components in all phases.

Therefore at equilibrium

$$0 = \Delta G^{\circ} + RT \ln \frac{\chi_B^Z \cdot \chi_A^W}{\chi_A^Z \cdot \chi_B^W}$$

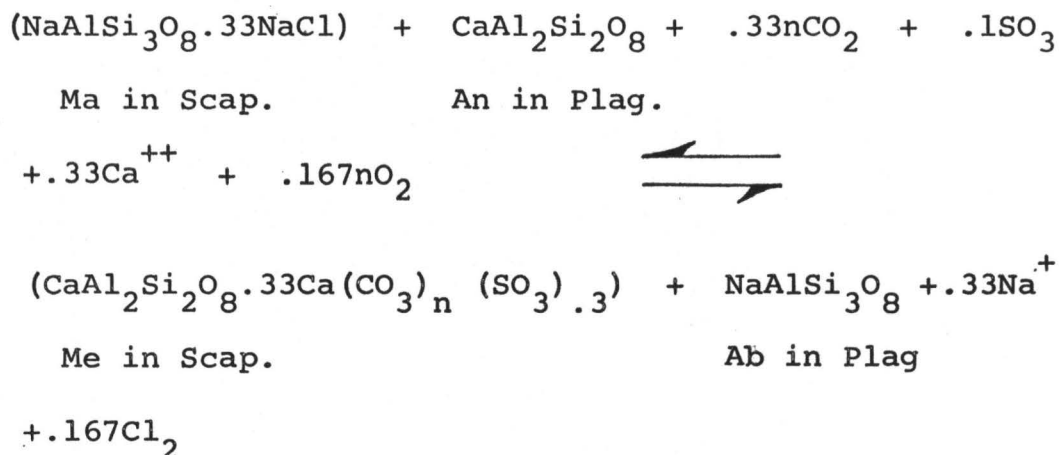
$$-\Delta G^{\circ} = RT \ln \frac{(1 - \chi_A^Z) \chi_A^W}{\chi_A^Z (1 - \chi_A^W)}$$

The expression

$$\frac{(1 - \chi_A^Z) \chi_A^W}{\chi_A^Z (1 - \chi_A^W)}$$

is recognized as the equilibrium constant.

The general case presented is that of a simple exchange reaction. The reaction between plagioclase and scapolite is however more complex. The reaction between these two minerals is presented as follows:



The equilibrium constant for the above reaction is written:

$$K = \frac{\overbrace{a_{\text{Me}}^{\text{Scap.}} \cdot a_{\text{Ab}}^{\text{Plag.}}}^{K'}}{\overbrace{a_{\text{Ma}}^{\text{Scap.}} \cdot a_{\text{An}}^{\text{Plag.}}}^{K''}} \cdot \frac{[f_{\text{Cl}_2}]^{.167} [a_{\text{Na}^+}]^{.33}}{[f_{\text{CO}_2}]^{.33n} [f_{\text{SO}_3}]^{.1} [f_{\text{O}_2}]^{.167n} [\bar{a}_{\text{Ca}^{2+}}]^{.33}}$$

The term K' may be further simplified assuming that $a \approx \text{Mole fraction} = \chi$

Therefore

$$K' = \frac{\chi_{\text{Me}}^{\text{Scap.}} (1 - \chi_{\text{An}}^{\text{Plag.}})}{(1 - \chi_{\text{Me}}^{\text{Scap.}}) \chi_{\text{An}}^{\text{Plag.}}}$$

where χ_{Me}^{scap} refers to the mole fraction of meionite in scapolite.

The value K' can be determined from probe studies (Table 10).

As may be seen from equation 1) the scapolite-plagioclase equilibrium is a function of fugacity of Cl_2 , CO_2 , SO_3 , and the activity of Na^+ and Ca^{2+} .

The range of K' (11.28 to 0.39) indicates that K'' is important in plagioclase-scapolite equilibrium reactions. From equation 1) the following conclusions may be reached:

1. Fugacity of CO_2 , Cl_2 and SO_3 influence the equilibrium between scapolite and plagioclase as do the variables temperature and pressure.
2. In particular, a CO_2 and SO_3 rich environment favours the stability of meionite and a Cl_2 rich environment favours the stability of marialite.
3. Diffusion of Ca^{2+} and Na^+ ions may be significant in establishing equilibrium between plagioclase and scapolite.

Discussion of Scapolite Analyses: The limits of scapolite composition of those samples analyzed by means of the probe are 17.2 and 83.5 mole per cent meionite. Pooling these data with those of D.M. Shaw

a histogram was obtained plotting frequency of analyses versus mole per cent meionite. Figure 26 illustrates that natural scapolite is restricted to the compositional limits of 17.2 and 84.9 mole per cent meionite. These per cent values are reasonably close to the 0 weight per cent intercepts for Cl (80.92 mole % Me) and SO_3 (15.36 mole % Me) as determined from linear regression curves; close enough to infer that these ions are controlling factors in the stability of scapolite.

Extremal States: From the graph plotting mole per cent meionite versus mole per cent anorthite, Figure 25 it is obvious that values representative of the anorthosite samples do not represent extremal values as predicted by Marakushev. This does not however disprove the existence of the extremal composition. To suitably investigate such a problem it would be necessary to study assemblages covering a wide and known range of intensive variables.

Wavelength Shift.

A comparison of the wavelength of $\text{SK}_{\alpha 1}$ in pyrite, marcasite, barium sulphite and barite suggests that the sulphur in scapolite occurs as sulphite. This study made in conjunction with H.P. Schwarcz was a preliminary

FIGURE 26

Mole % Meionite vs Frequency of Analysis.

The data for this histogram were obtained from probe analyses by the author and satisfactory analyses of scapolite obtained by D.M. Shaw. (1960).

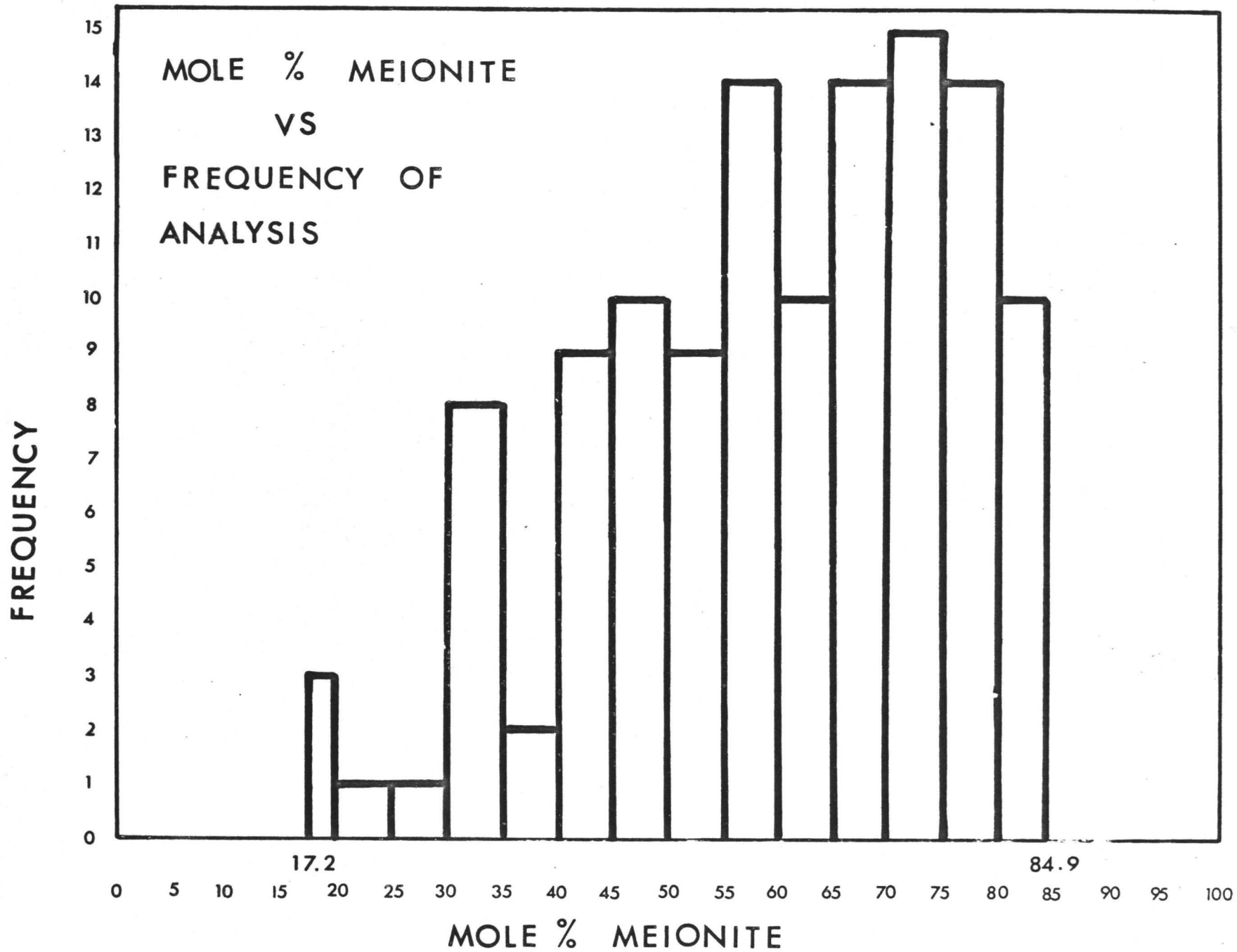


FIGURE 26

study on wavelength shift and must be refined to present quantitative data.

PETROLOGY

Petrogenesis of Scapolite.

Skarn zones, contact zones and pegmatitic areas all may be associated with an abundance of volatiles. These volatiles are undoubtedly important in the formation of scapolite. Textural evidence supports the assumption that scapolite in some cases may form as a result of diffusion of volatiles along fissures or crevices.

Plate 2 illustrates a preference for scapolite to form along fractures.



Plate 2: Anorthosite IM-3
Crossed nicols, illustrating initial stages of scapolitization

* For all photomicrographs Scale: 1 inch = 1.2 m.m.

However scapolite formation does not appear to be exclusively controlled by fracturing. Plate 3 illustrates an intersertal replacement texture in which scapolite is completely surrounded by plagioclase.



Plate 3: Anorthosite IM-3
Illustrating intersertal scapolitization, crossed nicols.

Undoubtedly nucleation sites have been provided by imperfections in minerals of these anorthositic rocks. The same rock types may show scapolite with a mosaic or equigranular texture (Plate 4).



Plate 4: Anorthosite S-44
Illustrating equigranular texture, final stages of
scapolitization, crossed nicols.

In former plates scapolite appears to be secondary in the latter primary. Plate 5 illustrates both a replacement and an equigranular texture. It is interesting to note the abundant inclusions of apatite in the plagioclase suggesting the abundance of volatiles during crystallization of the anorthosite. In all previous samples scapolite was less abundant than the other major minerals. Plate 6 illustrates an example of scapolite in abundance. This plate shows a granoblastic texture.



Plate 5: Anorthosite S-54
 Illustrating equigranular and replacement texture, crossed
 nicols.



Plate 6: Hornblende-Scapolite-Sphene-
 Plagioclase Gneiss, CA 76, crossed nicols.

Scapolite here abutts sharply against all minerals including plagioclase. Plate 7 illustrates a poikiloblastic texture.



Plate 7: Scapolite-Plagioclase-Hornblende Gneiss. Note poikiloblastic texture, crossed nicols.

The author has noted that in certain gneisses scapolite forms bands. This may indicate that either certain layers within the rock act as permeable layers conducting volatiles to nucleation sites thus allowing scapolite to form or that volatile rich sediments have held these volatiles until metamorphism resulted in the formation of scapolite bands. Plates 8 and 9 indicate the

formation of bands and stringers of scapolite in paramphibolite. (These photographs were contributed by D.M.Shaw.) These stringers and the bands of scapolite are probably representative of former diffusion paths for volatiles.

Zoning in skarns is commonplace. Previously, two zoned skarns have been mentioned. A third zoned skarn was observed by the author when accompanying D.M. Shaw on a field trip to the Haliburton area. The skarn was located in the Haliburton town quarry.



Plate 8: Paramphibolite
Illustrating stringers of scapolite.



Plate 9: Paramphibolite
Illustrating bands of scapolite.

The country rock, a dolomitic marble showed lineation parallel to the dip of the skarn zone. The zonal sequence was from the centre: scapolite, dolomite containing abundant clinopyroxene, and finally phlogopite. This type of zoning observed in the field in many skarn zones may be explained by diffusion of volatiles and other mobile elements. In the case of the Haliburton quarry skarn structural control is evident.

The source of volatiles resulting in the formation of scapolite is problematic. Volatile rich environments may be a result of intrusion of sediments or else high

grade metamorphism of such.

Mineral Facies.

From the mineral assemblages observed in scapolite bearing rocks a facies diagram was constructed. Figure 27 presents both AKF and ACF diagrams. The positions of the tie lines are strictly for the purpose of representing phase assemblages and are not intended to indicate more than an approximate mineral composition of any individual phase. The ACF diagram is essentially similar to that presented by D.M. Shaw (1960). However, biotite was included in preference to phlogopite as biotite is more abundant than the former mineral. It must be noted however that phlogopite is abundant in skarn type deposits. The presence of microcline coexisting with scapolite is indicated in the AKF diagram. The author also feels that this facies characterized by the sphene-diopside-scapolite assemblage is sufficiently unique and widespread in the Grenville-type rocks to justify classification as a separate subfacies of the amphibolite facies.

FIGURE 27

Facies Diagrams for Scapolite Assemblages.

ACF and AFK DIAGRAMS FOR SCAPOLITE ASSEMBLAGES

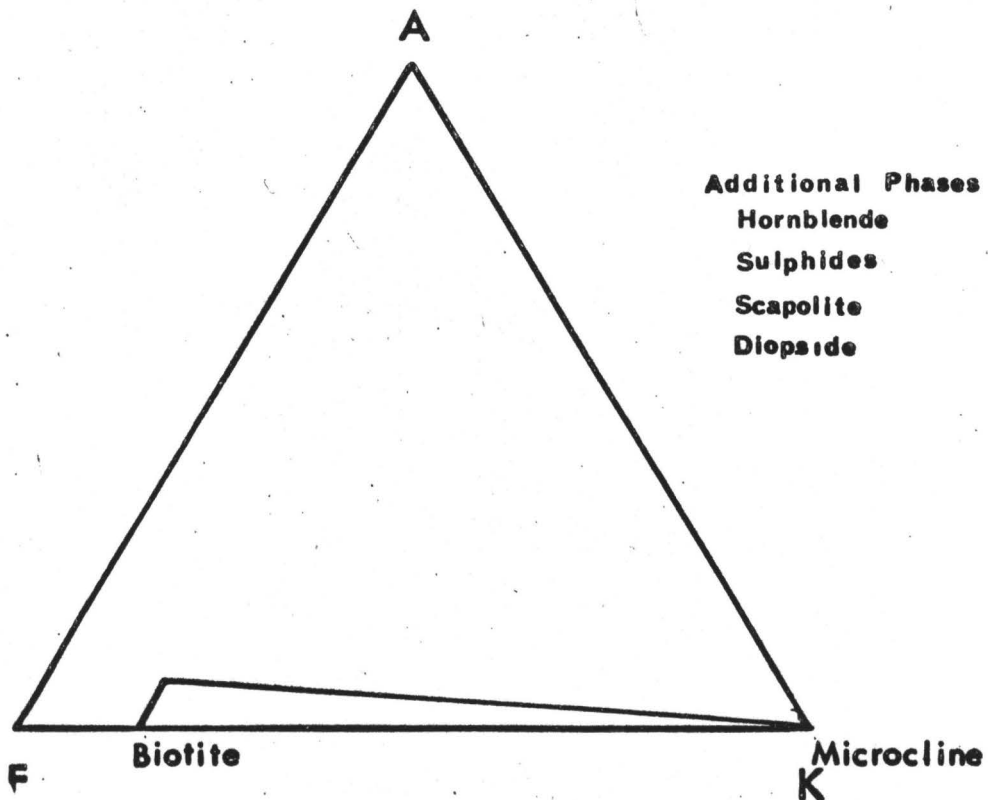
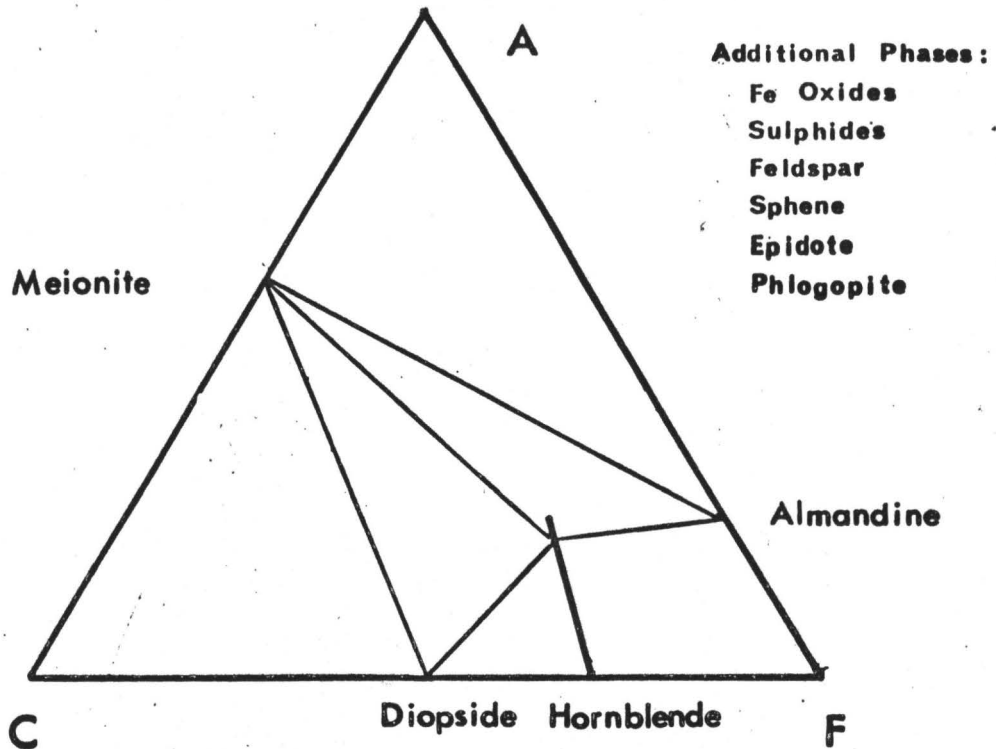


FIGURE 27

CONCLUSIONS

It has been illustrated clearly that the proportions of Na, Ca, Al, Si, CO₂, SO₃ and Cl vary in a regular manner either decreasing or increasing in an approximately linear fashion between the scapolite end members marialite and meionite. An intensive study involving specific gravity, refractive index and cell parameter determinations has further delineated, within reasonable limits the variation of physical properties with increasing mole per cent meionite.

One of the principal conclusions of this study is that scapolite stability limits appear to be reflected by the proportions of SO₃ and Cl.

Upon consideration of a possible reaction between scapolite and plagioclase it is concluded that f_{CO_2} , and f_{Cl_2} and f_{SO_3} are three important factors in the distribution of Ca between plagioclase and scapolite in an exchange reaction.

Probe studies have demonstrated that scapolite is generally more calcium rich than the coexisting plagioclase, and that the mole per cent meionite may

exceed the mole per cent anorthite generally by 20% and by as much as 50%.

Due to the large percentages of volatiles necessary for the formation of scapolite it may be stated that the presence of scapolite is indicative of a volatile rich "wet" environment, typified in the amphibolite facies by the assemblage sphene-pyroxene-scapolite.

BIBLIOGRAPHY

- Barth, T.F.W. 1952: Theoretical Petrology, New York,
J. Wiley and Sons, 416 P.
- Birks, L.S., 1963: Electron Probe Microanalysis,
Interscience.
- Burley, B.J., Freeman, E.B., and Shaw, D.M., 1961:
Studies on Scapolite, Canadian Min., v. 6,
P 670-678.
- Deer, Howie, and Zussman, 1963: Rock Forming Minerals,
New York, J. Wiley and Sons, v. 4, 435 P.
- Eugster, H.P., and Prostka, H.J. 1960: Synthetic
Scapolites, Bull. Geol. Soc. Amer., v. 71
P. 1859 (abstract).
- _____, _____. Appleman, D.E. 1962: Unit Cell
Dimensions of Natural and Synthetic Scapolites.,
Science, v. 137, no. 3533, P. 853-854.
- Fyfe, W.S., Turner, F.J., Verhoogen, J., 1958: Metamorphic
Reactions and Metamorphic Facies, Mem. Geol.
Soc. Amer. 73, 259 P.
- Harme, M. 1964: A Zoned Skarn Dike in Silrola, Southern
Finland, v. 37, P. 99-105.

- Lovering, J.F., White, A.J.R., 1964: The Significance of Primary Scapolite in Granulitic Inclusions from Deep-seated Pipes. Jour. Petrology, v. 5 P. 195-218.
- Marakushev A.A. 1964: Analysis of Scapolite Paragenesis Geochemistry International.
- Papike, J.J., 1964: The Crystal Structure and Crystal Chemistry of Scapolite, Unpublished Ph.D. Thesis, University of Minnesota.
- Schwarcz, H.P., Speelman, E.L., 1965: Determination of Sulfur and Carbon Coordination in Scapolite by Infra-red Absorption Spectrophotometry, American Mineralogist, v. 50 P. 656-666.
- Shaw, D.M. 1960: The Geochemistry of Scapolite, Part I Previous Work and General Mineralogy, Part II, Trace Elements, Petrology and General Geochemistry, Jour. Petrology, v. 1. P. 218-261.
- _____, Moxham, R.L., Filby, R.H., Lapkowsky W.W., 1963: Canadian Min. v. 7, P. 420-442.
- _____, Schwarcz, H.P., Sheppard, M.F., 1965; The Petrology of Two Zoned Scapolite Skarns, Can. Jour. of Earth Sciences, v. 2. P. 577-595.

- Smith J V., 1965: X-ray-Emission Microanalysis of Rock
Forming Minerals, I. Experimental Techniques,
Jour. Geol., v. 73, P. 830-864.
- _____, Ribbe, P.H. 1966: X-Ray Emission Microanalysis
of Rock Forming Minerals, IV Plagioclase
Feldspars, Jour. Geol., v. 74 P. 217-233.
- Turner, F.J., Verhoogen, J., 1951: Igneous and Metamorphic
Petrology, New York McGraw-Hill Inc., 694P.